Laser Induced Fluorescence and Transient Absorption Studies on the Excitation Energy Transfer of Free Radicals and Carbenes

博　士　論　文

Laser Induced Fluorescence and Transient Absorption Studies on the Excitation Energy Transfer of Free Radicals and Carbenes.

レーザー誘起蛍光及び過渡吸収分光法によるフリーラジカルと
カルベンの励起エネルギー移動に関する研究

甲　谷　　繁

平成９年３月

博　士　論　文

Laser Induced Fluorescence and Transient Absorption Studies on the Excitation Energy Transfer of Free Radicals and Carbenes.

レーザー誘起蛍光及び過渡吸収分光法によるフリーラジカルとカルベンの励起エネルギー移動に関する研究

金沢大学大学院自然科学研究科

甲谷　繁

CONTENTS

CHAPTER 1

INTRODUCTION

Introduction

Free radicals and carbenes are typical transient species in photochemical reactions. Free radicals are atoms or molecules that possess one or more unpaired electrons. Carbenes are the species with a divalent carbon atom which consists of two different electronic configurations for two nonbonding electrons, i.e., singlet and triplet. Paramagnetism is an important characteristic of free radicals and triplet carbenes.

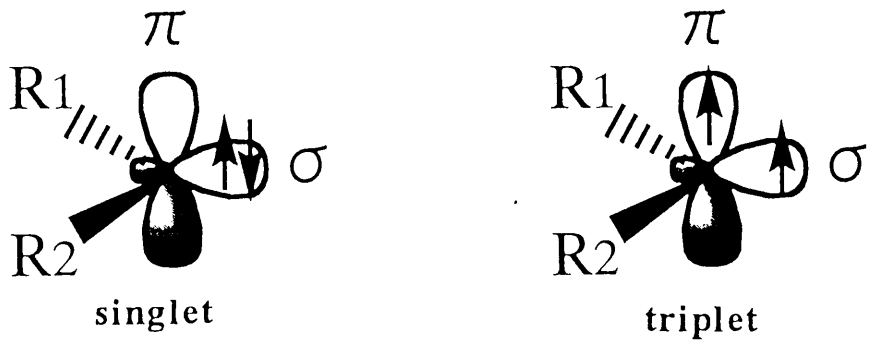

With the development of laser flash photolysis in 1960's, numerous investigations of direct spectral observation for short-lived intermediates have been reported. There are various methods for detecting such short-lived species by using pulsed lasers with nano- and picosecond time duration.[1,2] Free radicals and triplet carbenes have been also extensively studied by electron paramagnetic resonance (EPR) spectroscopy including recent time-resolved ESR spectroscopy.[3,4] These methods provide us with a great amount of information about molecular geometry, electronic structures and reaction dynamics.[4,5]

Recent interest is directed toward investigating physical and chemical interactions of free radicals and carbenes with other molecules. In photochemistry, numerous investigations of bimolecular processes such as electronic energy transfer[6-9], the excited-state complex formations[10,11], and photoinduced electron transfer[12] have been reported. In the case where free radicals and/or carbenes involved, however, there are a few studies on photophysical bimolecular processes, especially for electronic energy transfer, because of instability of these species in solution.

Electronic energy transfer is one of the important process in photochemistry. Most energy transfer can be described by

$$D^* + A \rightarrow D + A^*. \qquad (1)$$

This process is observed at the earlier stage of photosynthetic reaction in plants or photosynthetic bacteria.[13] Solar energy conversion begins with the capture of sunlight by hundreds of chlorophyll array and the efficient energy transfer toward a reaction center is followed. The transfer mechanism is mainly due to Coulombic dipole-dipole interaction which was theoretically developed by Förster and others.[6-9] In this theory, critical transfer distance, R_0, is defined as a mean distance between donor and acceptor where the rate constant for resonance energy transfer is equal to the sum of rate constants for all other donor deexcitation processes in the absence of acceptors. The quantity R_0 is useful in evaluating the effectiveness of the

resonance energy transfer.

Triplet-triplet fluorescence of diphenylcarbene (DPC) and its derivatives in low-temperature matrix have attracted special interest. The fluorescence of these carbenes clearly shows nonexponential decay curves and they are modified in the presence of a magnetic field.[14] Owing to paramagnetism of triplet carbenes, the fluorescent state (T_1) of DPC is influenced by internal and external magnetic fields. In order to understand the interaction between electron spin and magnetic fields, i.e. spin-orbit coupling and external magnetic field effects in the excited DPC, the characterization of the T_1 sublevels is an important matter. Further, magnetic field effects on a coupling reaction of two carbenes seem to be an interesting subject but have not been reported at all. Contrary to this situation, there are so many reports for the magnetic field effects on radical recombination reactions.[15-17]

In this thesis, the author deals with the three interesting and unsolved topics concerning with aromatic free radicals and carbenes: (1) quantitative evaluation of intermolecular electronic energy transfer on the basis of the Förster theory, (2) spin-orbit coupling induced intersystem crossing process in the excited states of DPC, and (3) magnetic field effects on a pair of diphenylcarbene moieties generated in the bichromophoric system.

In order to demonstrate the validity of Förster theory for the energy transfer participating a free radical as energy

acceptor, in chapter 2, fluorescence quenching of dye molecules by 2,4,6-tri-*tert*-butylphenoxyl radical (TBPR) is presented. TBPR is a suitable free radical for studying resonance energy transfer quantitatively, because this radical is stable even in solutions at room temperature[18] and has relatively strong and broad absorption band in visible region.

In chapter 3, resonance energy transfer from the excited triplet state T_1 of DPC to dye molecules is described. Here, the author suggests that the resonance energy transfer is a powerful tool for characterization of the T_1 sublevels of DPC which cannot be obtained by an ordinary spectroscopy. The energy transfer analysis applied for the quenched fluorescence decay curves of DPC will be considered as an excellent method to investigate the rates of deactivation processes in the triplet excited state T_1.

In chapter 4, effects of pulsed laser intensity and magnetic fields on the primary photochemical process in 1,8-bis[4-(α-diazobenzoyl)phenoxyl]octane (BDO) is considered. On the high density pulsed laser excitation, two diphenylcarbene moieties on the both ends of alkyl chain can be simultaneously generated from BDO. It is demonstrated that the biphotonic reaction are well controlled by pulsed laser intensity and magnetic fields.

References

(1) Fleming, G. R. *Chemical Application of Ultrafast Spectroscopy,* Oxford University Press, New York, 1986.

(2) Brückner, V.; Feller, K. H. ; Grummt U. W. *Applications of Time-resolved Optical Spectroscopy*, Elsevier, Amsterdam, 1990.

(3) *Advanced EPR - Applications in Biology and Biochemistry* - (ed. Hoff, A. J.) Elsevier, Amsterdam, 1989.

(4) *Spin Chemistry - Spin Polarization and Magnetic Field Effects in Photochemical Reactions* - (ed. I'Haya, Y. J.), The Oji International Conference, 1991; references therein.

(5) *Handbook of Organic Photochemistry* (ed. Scaiano, J. C.) CRC Press, Boca Raton, 1989; Volume 1, 2.

(6) Förster, T. *Discuss. Faraday Soc.* 1959, *27*, 7.

(7) Dexter, D. L. *J. Chem. Phys.*, 1953, *21*, 836.

(8) Lamola, A. A. ; Turro N. J. *Energy Transfer and Organic Photochemistry*, Wiley, New York, 1969; Chapter 2.

(9) Berlman, I. B. *Energy Transfer Parameters of Aromatic Compounds*, Academic Press, New York, 1973.

(10) *Organic Molecular Photophysics* (ed. Birks J. B.), Wiley, New York, 1975; Volume 2 Chapter 9.

(11) (a) Ware, W. R.; Watt, D.; Holmes, J. D. *J. Am. Chem. Soc.* 1974, *96*, 7853. (b) Ware, W. R.; Holmes, J. D.; Arnold D. R. *J. Am. Chem. Soc.* 1974, *96*, 7861.

(12) Marcus, R. A.; Sutin N. *Biochem. Biophys. Acta* 1985, *811*, 265.

(13) Barber J.; Andersson B. *Nature* 1994, *370*, 31.

(14)(a) Haider, K. W.;Platz, M. S.;Despres, A.; Lejeune, V.; Migirdicyan, E. *J. Phys. Chem.* 1990, *94*, 142. (b) Despres, A.;Lejeune, V.;Migirdicyan, E.;Platz, M. S. *J. Phys. Chem.* 1992, *96*, 2486. (c) Despres, A.;Lejeune, V.;Migirdicyan, E.;Admasu, A.;Platz, M. S.; Berthier, G.; Parisel, O.; Flament, J. P.; Baraldi, I.; Momicchioli, F. *J. Phys. Chem.* 1993, *97*, 13358. (d) Kozankiewicz, B.;Despres, A.;Lejeune, V.;Migirdicyan, E.; Olson, D.; Michalak, J.;Platz, M. S. *J. Phys. Chem.* 1994, *98*, 10419.

(15) *Spin Polarization and Magnetic Effects in Radical Reactions* (ed. Molin, Yu. N.), Elsevier, Amsterdam, 1984.

(16) Doubleday Jr., C.; Turro N. J.; Wang J. F. *Acc. Chem. Res.* 1989, *22*, 199.

(17) Steiner, U.; Ulrich, T. *Chem. Rev.*, 1989, *89*, 51

(18) Denisov, E. T.; Khudyakov I. V. *Chem. Rev.* 1987, *87*, 1313.

CHAPTER 2

RESONANCE ENERGY TRANSFER FROM THE EXCITED SINGLET STATE OF DYE MOLECULES TO A STABLE FREE RADICAL

2.1 Abstract

Fluorescence quenching of dye molecules such as Coumarin 153, DCM, and nile red by the stable 2,4,6-tri-*tert*-butylphenoxyl radical in an MTHF glass matrix at 77 K was studied by means of subnanosecond time-resolved fluorescence spectroscopy. The quenching process is ascribed to the dipole-dipole interaction amenable to Förster theory. The average critical energy transfer distances were determined to be 2.0, 2.7, and 3.1 nm for Coumarin 153, DCM, and nile red, respectively. These values are consistent with those evaluated from spectroscopic data.

2.2 Introduction

Free radicals possess great ability to interact with aromatic molecules which results in the quenching of their excited states. Several mechanisms have been considered in the excited state quenching by free radicals: e.g. energy transfer of Förster type or Dexter type, electron transfer, electron exchange induced relaxation processes (intersystem crossing and internal conversion). In the case of excited singlet state quenching, it is expected that the Förster energy transfer according to

$$^1D^* + {}^2A \rightarrow {}^1D + {}^2A^*$$

efficiently occurs because both the radiative transition $^1D^* \rightarrow {}^1D$ and the absorptive transition $^2A \rightarrow {}^2A^*$ are spin allowed. However, there has been few reports to confirm this quenching process quantitatively, because the high reactivity and instability of the radicals prevent the exact determination of their concentrations. Therefore, stable free radicals are suited to the study of the Förster energy transfer from an excited singlet state molecule to a free radical.

Nitroxyl radicals such as 2,2,6,6-tetramethyl-1-piperidinyloxy and di-*tert*-butyl nitroxide which are stable even at room temperature are the best known quenchers of excited singlet state molecules.[1-6] However, a Förster-type energy transfer has been suggested to be insignificant in these systems because of the low extinction coefficients of nitroxyls (460 nm, $\varepsilon \sim 10$ $M^{-1}cm^{-1}$). To the best of the author's knowledge, only the

stable diphenylpicrylhydrazyl radical has been proven to act as the fluorescence quencher in the Förster-type energy transfer by means of steady-state fluorescence measurements.[7]

In this study, fluorescence decay curves of dye molecules, 2,3,5,6-1H,4H-tetrahydro-8-trifluoromethylquinolizino-<9,9a,1-gh> coumarin (coumarin 153), 4-dicyanomethylene-2-methyl-6-(p-dimetylaminostylyl)-4H-pyran (DCM), and 5-amino-9-diethyliminobenzo(a)phenoxazone (nile red) quenched by 2,4,6-tri-*tert*-butylphenoxyl radical (TBPR) in 2-methyltetrahydrofuran (MTHF) at 77 K were measured by means of subnanosecond time-resolved fluorescence spectroscopy. The stable TBPR was chosen as an energy acceptor because it has a relatively strong and broad absorption band (λ_{max} = 625 nm, ε_{max} = 420 $M^{-1}cm^{-1}$) as shown in Fig. 2. The Förster-type energy transfer leads to non-exponential time dependence of the donor fluorescence decay which gives us the critical energy transfer distance (R_0). The values of R_0 determined from fluorescence decay curves are compared with those estimated from a calculation of spectral overlap.

2.3 Experimental Section

Coumarin 153 (Lambda Physik), DCM (Lambda Physik) and nile red (Aldrich) were used without further purification. MTHF (Tokyo Kasei), washed with 10% NaOH and dried over $MgSO_4$, was subjected to fractional distillation over CaH_2 followed by distillation over potassium metal. TBPR was prepared by treating 2,4,6-tri-*tert*-butylphenol (Tokyo Kasei) with PbO_2 powder (0.15 g / 5 ml) in degassed MTHF under vigorous stirring. The solution was filtrated through a glass filter to remove PbO_2 powder. The radical solution ($\sim$0.1 mM) thus obtained was mixed with a degassed dye solution. Finally, the mixed solution was transferred into a quartz cell (1 mm optical pathlength) and sealed off. All these procedures were performed in the vacuum condition ($\sim 10^{-3}$ Torr), since TBPR is gradually oxidized in aerated solution. Concentrations of TBPR were calculated from the absorbance and molar extinction coefficient at 625 nm. The value of ϵ_{625} in MTHF at 77K was determined to be 420 ± 13 $M^{-1}cm^{-1}$ by the reported method.[8]

Figure 1 shows the experimental setup for a measurement of a subnanosecond time-resolved fluorescence. The hydrogen Raman-shifted second harmonic (436 nm) of a pulsed Nd:YAG laser (Coherent Antares 76-s/Continuum RGA 60; 100 ps pulse width, 10 Hz repetition rate) was used for photoexcitation. The fluorescence of DCM and that of Coumarin 153 were observed through a polychromator with 100 grooves/mm grating (Jobin Yvon

HR250). Time-Resolved detection was performed with a photon-counting streak camera (Hamamatsu Photonics C2050/M1952)/CCD temporal analyzer (3140-69) system interfaced with a Hamamatsu C3366 I/F unit. The fluorescence of nile red, selected at 580 nm by a monochromator (Ritsu MC-20L), was detected by a photo-multiplier (Hamamatsu H-3284). Signals from the photomultiplier were recorded on a digital storage oscilloscope (Tektronix TDS-520) interfaced to a personal computer (NEC PC9801).

2.4 Results and Discussion

2.4.1 Critical energy transfer distances calculated from spectroscopic data

According to the Förster theory[9], R_0 can be expressed by

$$R_0^6 = \frac{9000(\ln 10)\,\kappa^2\,\phi_D}{128\,\pi^5 n^4 N}\,J \qquad (1)$$

where κ^2 and ϕ_D are the orientation factor and fluorescence quantum yield of donor in the absence of energy transfer, respectively: n and N are the refractive index of the medium and Avogadro's number, respectively. J is the Förster overlap integral as expressed by

$$J = \int \frac{F_D(\tilde{\nu})\,\varepsilon_A(\tilde{\nu})}{\tilde{\nu}^4}\,d\tilde{\nu} \qquad (2)$$

$F_D(\tilde{\nu})$ and $\varepsilon_A(\tilde{\nu})$ are the spectra of donor emission normalized to unity and the molar extinction coefficient of acceptor, respectively.

The fluorescence spectra of the dye molecules (Coumarin 153, DCM and nile red) and the absorption spectrum of TBPR are shown in Figure 2. The absorption band of TBPR around 625 nm is so broad that the spectral overlap between the fluorescence of the dye molecules and the absorption of TBPR is significant. The values of R_0 calculated from eq. 1 and 2 are 1.9, 2.5, and 2.8 nm for Coumarin 153, DCM, and nile red, respectively. These values are summarized in Table 1.

The values of ϕ_D for Coumarin 153, DCM, and nile red are

also listed in Table 1. These values are obtained by the relation of $\phi_D = k_r \cdot \tau_1$, where k_r and τ_1 are the radiative rate constant and the fluorescence lifetime of dye molecules. k_r was calculated from the Strickler-Berg equation[10] and τ_1 was determined by analyzing the fluorescence decay of dye molecules in the absence of TBPR as mentioned later. Calculated k_r values are sufficiently reliable because these dye molecules satisfy the following two requirements described in reference 10: (1) large extinction coefficient (more than 8000 $M^{-1}cm^{-1}$); (2) unchanging configuration in the excited state. The value $\kappa^2 = 0.476$ is quoted for a rigid random orientation. The value of n for MTHF at 77 K has not been reported so far; therefore, this value is determined to be 1.43 using n = 1.405 at 293 K and its temperature dependence $dn/dT = -10^{-4}\ K^{-1}$.[11]

2.4.2 Fluorescence quenching of dye molecules

Since TBPR is non-fluorescent, the quenching mechanism could not be determined by measuring the doublet-doublet fluorescence of TBPR. The author therefore tried to prove it by time-resolved fluorescence measurements of the dye molecules. A 436 nm subnanosecond pulse was used as excitation light, because the absorption intensity of TBPR is negligible at this wavelength (436 nm). However, the molar extinction coefficient of nile red is also small at 436 nm. Consequently, the fluorescence of nile

red was detected by a highly sensitive photomultiplier instead of the streak camera.

Fluorescence decay curves of Coumarin 153, DCM, and nile red in the presence of various concentrations of TBPR are shown in Figures 3 - 5, respectively. The fluorescence intensities at the time origin are nearly normalized. The fluorescence lifetimes of Coumarin 153, DCM and nile red in the absence of TBPR were 5.3, 2.2 and 4.7 ns, respectively, as will be mentioned later. Apparent fluorescence lifetime decreases with increasing TBPR concentration. These results clearly indicate that the lowest excited singlet state (S_1) of dye molecules are quenched by TBPR.

The fluorescence of DCM and nile red are efficiently quenched by TBPR, whereas the fluorescence of Coumarin 153 is not so efficiently quenched even at the highest concentration (57.1 mM) of TBPR. This result is consistent with the fact that the R_0 value of Coumarin 153 determined from spectroscopic data is the smallest of those of the three dye molecules. The Förster-type energy transfer is therefore the most probable quenching mechanism.

The fluorescence decay of the donor undergoing dipole-dipole resonance energy transfer in uniformly distributed and randomly oriented system is expressed by[12]

$$I(t) = A \exp[-t/\tau_1 - X(t/\tau_1)^{1/2}] \quad (3)$$

where τ_1 is the fluorescence lifetime of the donor in the absence of TBPR and

$$X = g(4/3000)\,\pi^{3/2} N C_A R_0^{3} \qquad (4)$$

in which g is the orientation factor, C_A is the concentration of acceptor, N is Avogadro's number and R_0 is the critical energy transfer distance. However, the observed fluorescence signals involved rise and decay components, they could not be fitted by eq. 3 which involves only the decay process. The term reflecting fluorescence rise may be introduced by taking into account the vibrational relaxation from upper vibronic levels to the lowest one in S_1 of the donor. Considering such a vibrational relaxation, the temporal behavior of the donor fluorescence is expressed by[13]

$$I(t) = A \int_0^t \exp\left[- \frac{t-u}{\tau_2} - \frac{u}{\tau_1} - X \left(\frac{u}{\tau_1} \right)^{\frac{1}{2}} \right] du \qquad (5)$$

where u is an integration variable with the dimension of time and τ_2 is a time constant of the vibrational relaxation.

Calculated fluorescence curves were obtained by the convolution method using the parameters A, τ_1, τ_2, and X. The set of parameters was found by a non-linear least-squares method so that the calculated curve makes the best fit to the observed curve. X can be set to zero for fluorescence curve measured in the absence of TBPR. All the parameters were determined for fluorescence curves measured in the presence of TBPR. Figure 6 shows a logarithmic plot of the fluorescence signal (dotted curve) of DCM in the presence of 21.6 mM TBPR. The decay curve

clearly shows a non-exponential decay. A solid curve, calculated from eq. 5 by using parameters (τ_1 = 2.2 ns, τ_2 = 0.04 ns and X = 1.80) fits the observed one well. Other fluorescence decay curves in the presence of TBPR were also fitted well by using the parameters summarized in Table 2. R_0 can be calculated from eq. 4, where g for rigid random orientation is 0.845. The values of R_0 are also listed in Table 2.

Three important features are found for fluorescence quenching of the three dye molecules in Table 2. (1) The values of τ_1 in the presence of various concentrations of TBPR are in good agreement with the fluorescence lifetime of dye molecules in the absence of TBPR (C_A = 0 mM). (2) The values of R_0 derived from X were nearly constant, since X increases linearly with increasing TBPR concentration as indicated by eq. 4. (3) The average values of R_0 for Coumarin 153/TBPR, DCM/TBPR, and nile red/TBPR combinations (2.0, 2.7, and 3.1 nm) are in good agreement with those (1.9, 2.5, and 2.8 nm) estimated from the spectral overlap.

These three features clearly indicate that the resonance energy transfer with dipole-dipole interaction is responsible for the fluorescence quenching of dye molecules (Coumarin 153, DCM and Nile Red) by TBPR. Furthermore, they also show that other processes such as electron transfer and/or electron exchange are never included. If other quenching mechanisms play an important role, the three characteristic features described above cannot be obtained. The fluorescence decay functions responsible for the

electron transfer and the electron exchange quenching are different from that responsible for the dipole-dipole energy transfer quenching.[14]

Empirically, the distance dependence of the electron transfer rate constant in frozen media is expressed by

$$k(r) = k_0 \exp[-\beta(r-r_0)] \qquad (6)$$

where r is the center to center distance between donor and acceptor, r_0 is a small connection for their radii, and the constant β is about 11 - 12 nm^{-1} for aromatic systems.[15] The largest rate (k_0) is usually thought to be close to the frequency of a single molecular vibration, 10^{13} s^{-1}. In the systems studied, the value of r is 1.9 nm even in the highest concentration (57.1 mM) of TBPR and the value of r_0 is about 0.5 - 0.7 nm. Consequently, the largest value of k(r) is approximately estimated to be 1×10^7 s^{-1}. Thus, the long-distance electron transfer in the nanosecond time region has a small possibility. The electron exchange mechanism is also negligible, because the limiting distance for the occurrence of electron exchange is usually shorter than that of electron transfer.

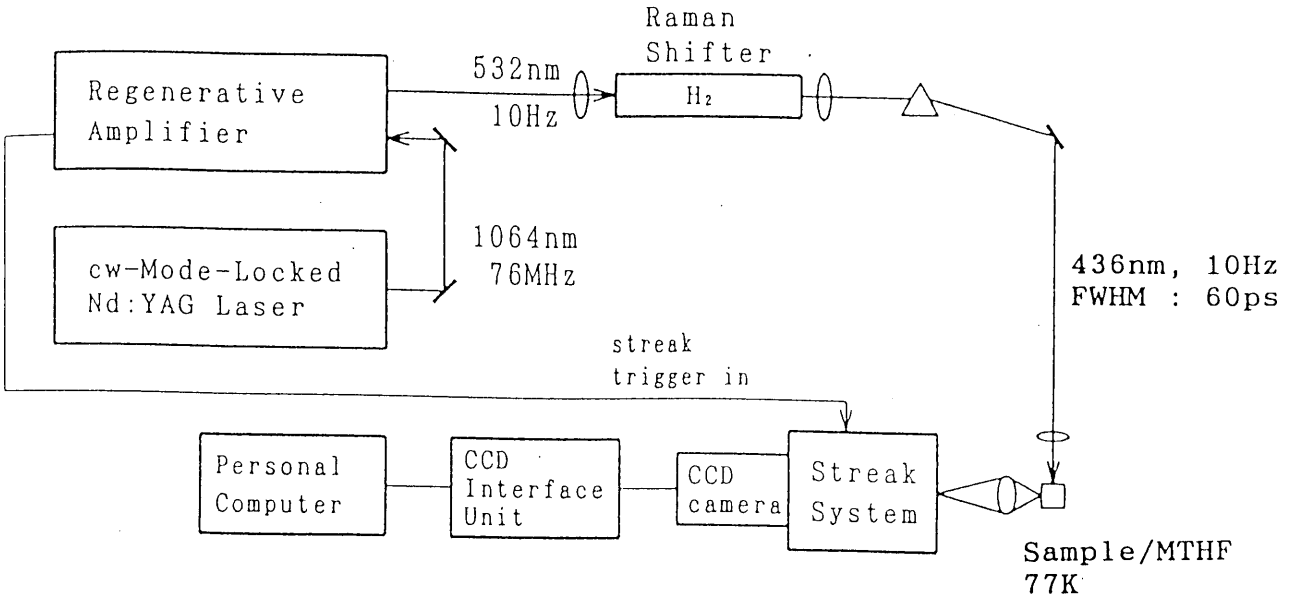

Figure 1. Experimental Setup for a measurement of a subnanosecond time-resolved fluorescence.

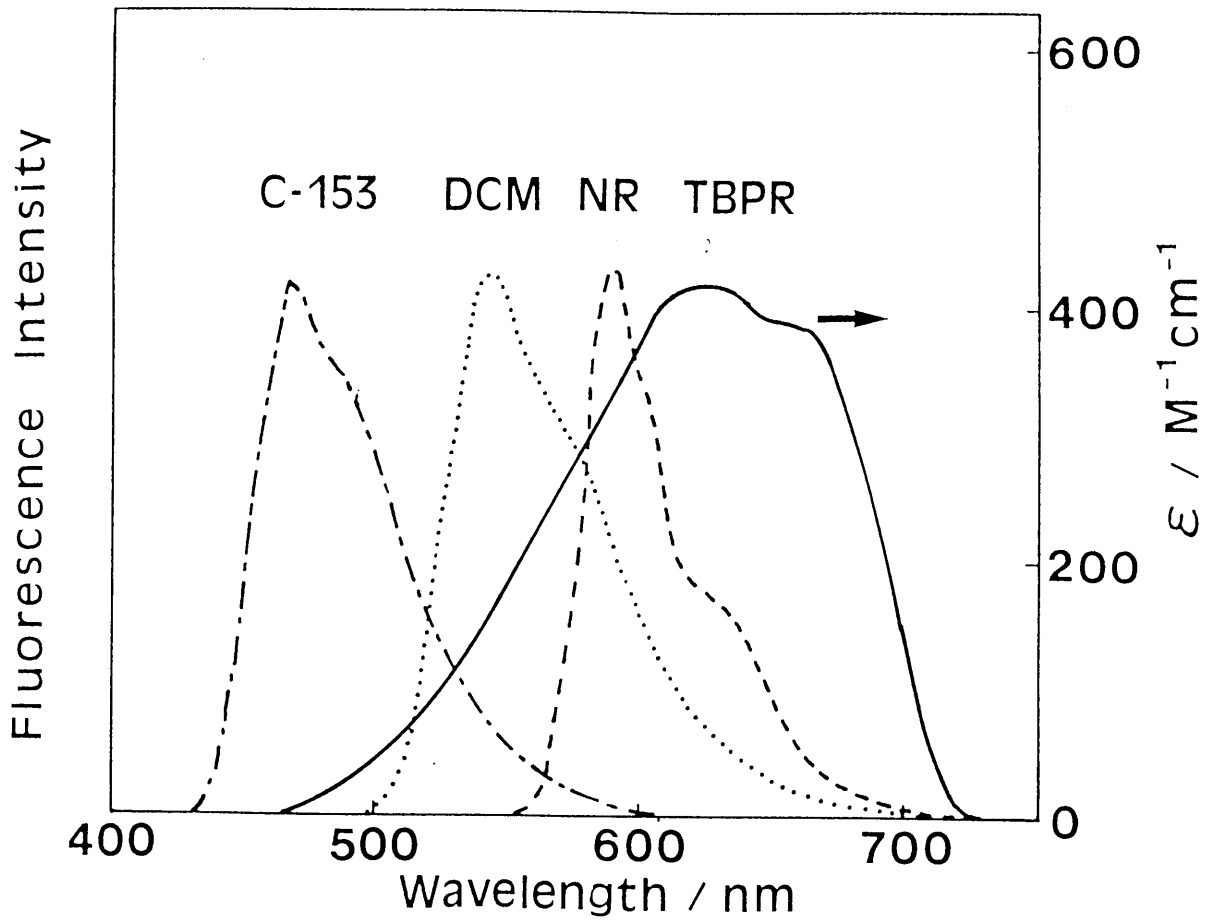

Figure 2. Fluorescence spectra of Coumarin 153 (C-153), DCM, nile red (NR) and absorption spectrum of 2,4,6-tri-*tert*-butylphenoxyl radical (TBPR).

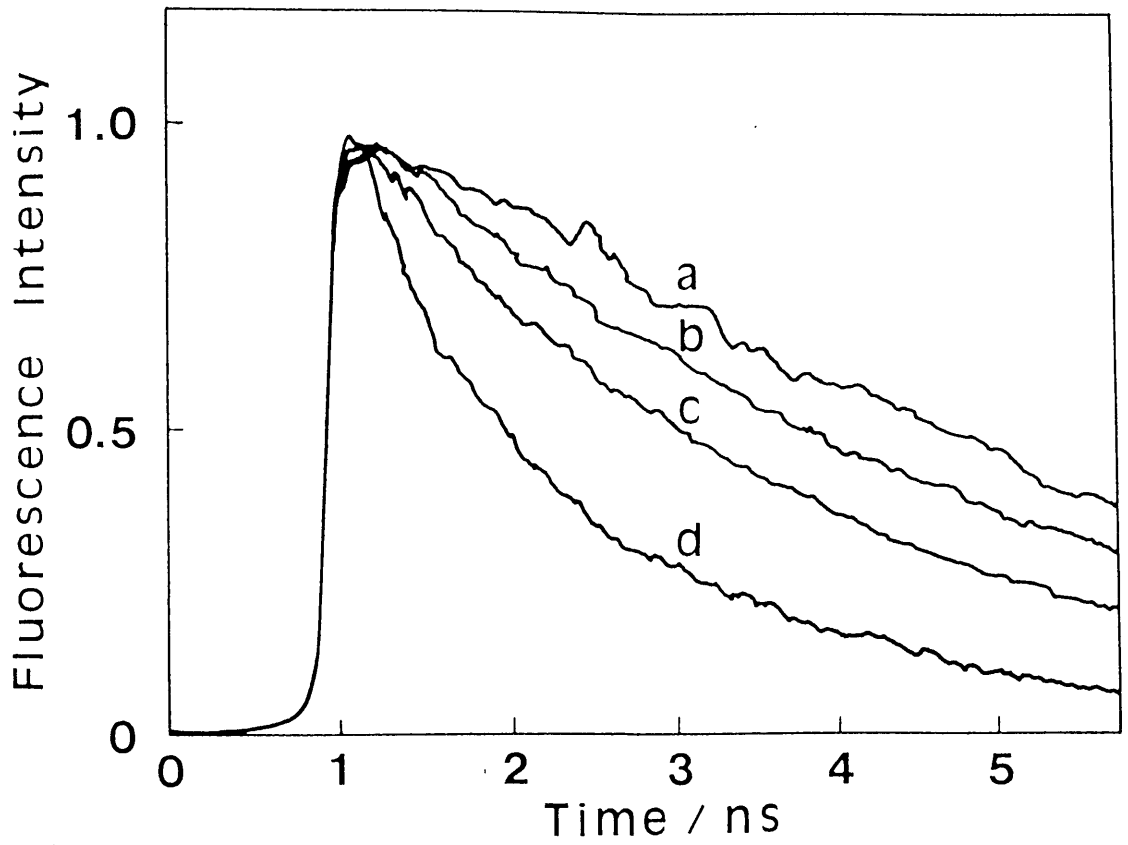

Figure 3. Fluorescence decay curves of Coumarin 153 in MTHF with (a) 0, (b) 9.7, (c) 25.4, and (d) 57.1 mM TBPR at 77 K.

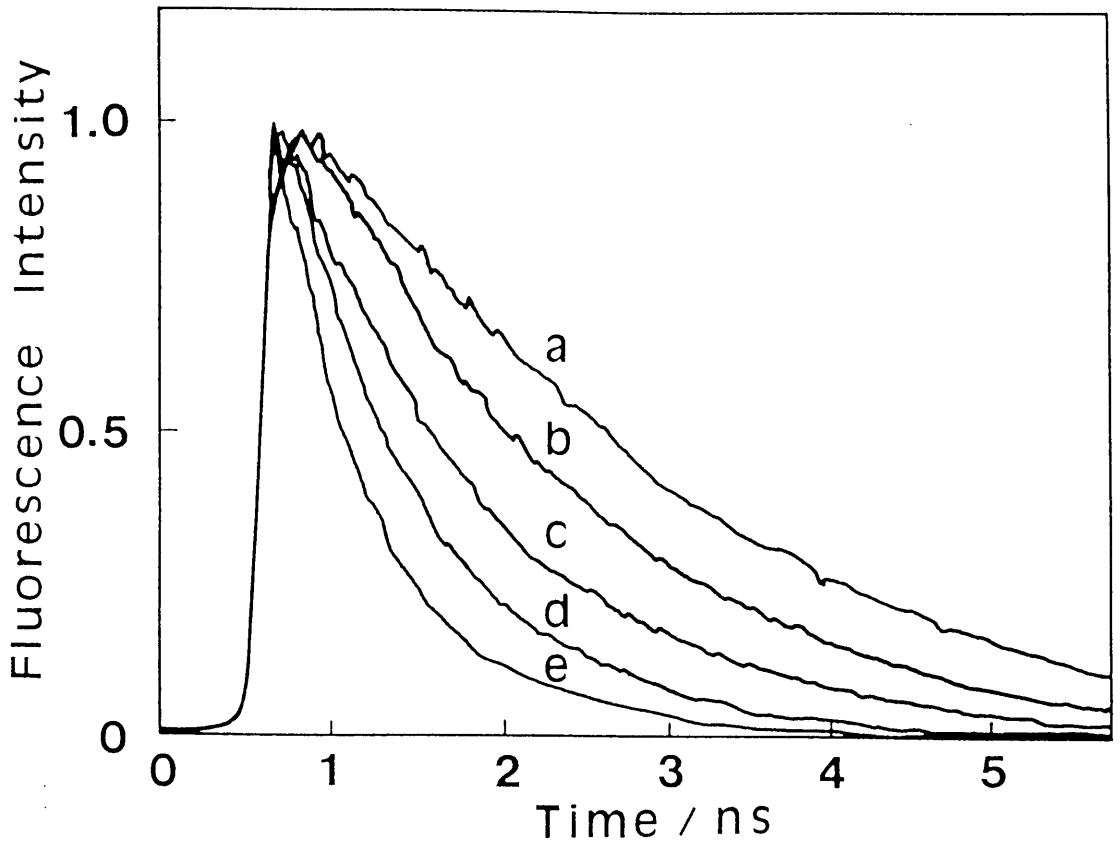

Figure 4. Fluorescence decay curves of DCM in MTHF with (a) 0 (b) 6.0, (c) 12.4, (d) 21.6, and (e) 32.1 mM TBPR at 77 K.

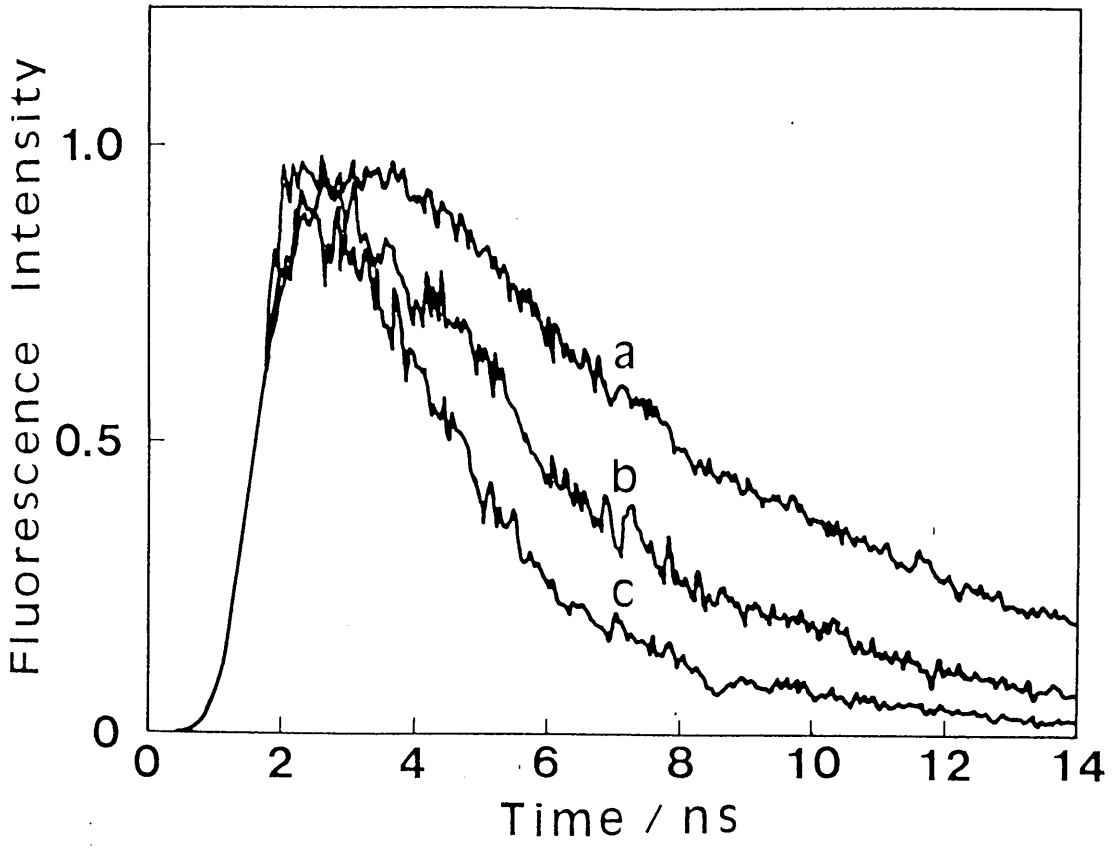

Figure 5. Fluorescence decay curves of Nile Red in MTHF with (a) 0, (b) 9.6 and (c) 19.3 mM TBPR at 77 K.

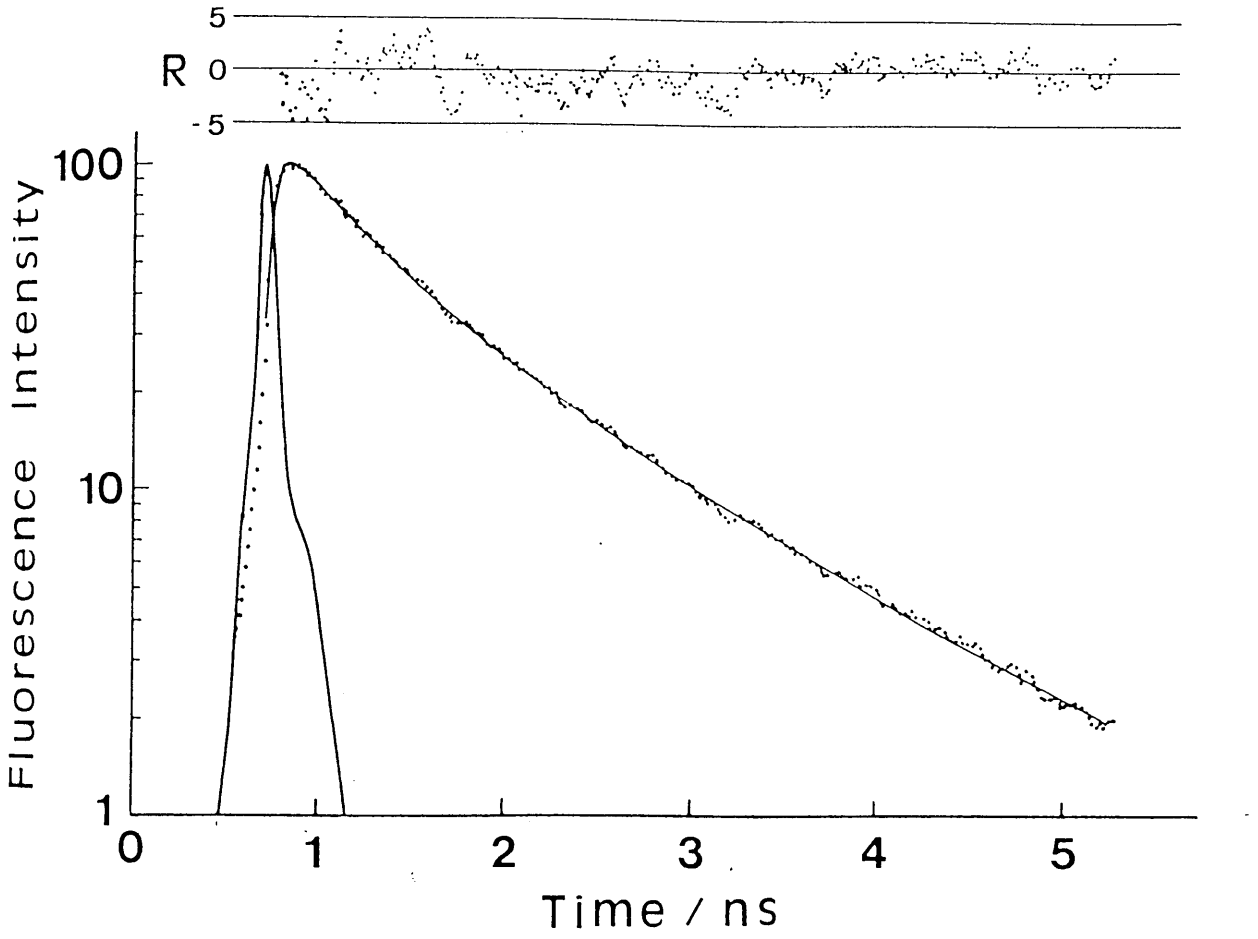

Figure 6. A logarithmic plot of the fluorescence intensity of DCM as a function of time for 21.6 mM TBPR in MTHF at 77 K. The solid curve was calculated from eq. 5 by using parameters: τ_1 = 2.2 ns, τ_2 = 0.04 ns and X = 1.80.

TABLE 1. Parameters for energy transfer from dye molecules to 2,4,6-tri-*tert*-butylphenoxyl radical (TBPR).

donor molecule	$10^{-16} J$ a) / $mol^{-1}cm^6$	$10^8 k_r$ b) / s^{-1}	τ_0 c) / ns	ϕ_D d)	R_0 e) / nm
Coumarin 153	4.6	1.75	5.3	0.93	1.9
DCM	28.4	3.32	2.2	0.74	2.5
Nile Red	48.4	2.00	4.7	0.94	2.8

a) The spectral overlap between fluorescence of dye molecules and absorption of TBPR.

b) Calculated by the Strickler-Berg equation.

c) Obtained form the fluorescence decay curves in the absence of TBPR.

d) $\phi_D = k_r \cdot \tau_0$.

e) Calculated from Eq. 1.

TABLE 2. Parameters for analysis of fluorescence decay curves of dye molecules undergoing the energy transfer to 2,4,6-tert-butylphenoxyl radical (TBPR).

Donor:Coumarin 153

C_A/mM	τ_1/ns	τ_2/ns	X	R_0/nm
0	5.3	0.07	-	-
9.7	4.9	0.05	0.30	2.0
25.4	5.0	0.04	0.80	2.0
57.1	5.3	0.03	2.12	2.1

Donor:DCM

C_A/mM	τ_1/ns	τ_2/ns	X	R_0/nm
0	2.2	0.06	-	-
6.0	2.1	0.06	0.39	2.6
12.4	2.0	0.04	0.88	2.7
21.6	2.2	0.04	1.80	2.8
32.1	2.2	0.03	2.80	2.8

Donor:Nile Red

C_A/mM	τ_1/ns	τ_2/ns	X	R_0/nm
0	4.7	0.03	-	-
9.6	4.5	0.03	0.93	3.0
19.3	4.8	0.02	2.30	3.2

C_A is the concentration of TBPR.

R_0 is calculated from Eq. 4

References

(1) Green, S. A.; Simpson, D.J.: Zhou, G.; Ho, P. S.; Blough N.V. *J. Am. Chem. Soc.*, 1990, *112*, 7337.

(2) Darmanyan, A. P.; Tatikolov, A. S. *J. Photochem.*, 1986, *32*, 157.

(3) Chattopadhyay, S. K.; Das, P. K.; Zhou, G.; Ho, P. S.; Blough, N. V. *J. Am. Chem. Soc.*, 1983, *105*, 6205.

(4) Kuzmin, V. A.; Tatikolov, S. A. *Chem. Phys. Lett.*, 1977, *51*, 45.

(5) Watkins, A. R. *Chem. Phys. Lett.*, 1974, *29*, 526.

(6) Green, J. A.; Singer, L. A.; Park, J. H. *J. Chem. Phys.*, 1973, *58*, 2690.

(7) Lisovskaya, I. A.; Plotonikov, V. G.; Alfimov, M. V. *Opt. Spectrosc.*, 1973, *35*, 634.

(8) Cook, C.D.; Norcross, B. E. *J. Am. Chem. Soc.*, 1959, *81*, 1176.

(9) Forster, T. *Discuss. Faraday Soc.*, 1959, *27*, 7.

(10) Strickler, S. J.; Berg, R. A. *J. Chem. Phys.*, 1962, *37*, 814.

(11) Perrin, D. D.; Armarego, W. L. F.; Perrin, D. R. *Purification of laboratory Chemicals*; Pergamon, Oxford, 1980.

(12) Lamola, A. A.; Turro, N. J. *Energy Transfer and Organic Photochemistry*, Wiley, New York, 1969; p 41.

(13) Lu, P. Y.; Yu, Z. X.; Alfano, R. R.; Gestern, J. I. *Phys. Rev. A*, 1982, *26*, 3610.

(14) Inokuti M.; Hirayama, F. *J. Chem. Phys.*, 1965, *43*, 1978.

(15) Marcus R. A.; Sutin, N. *Biochem. Biophys. Acta*, 1985, *811*, 265 and references therein.

LIST OF COMPOUNDS

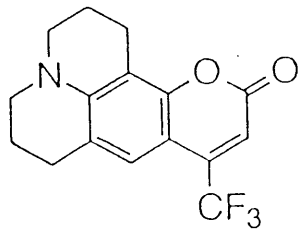

C-153

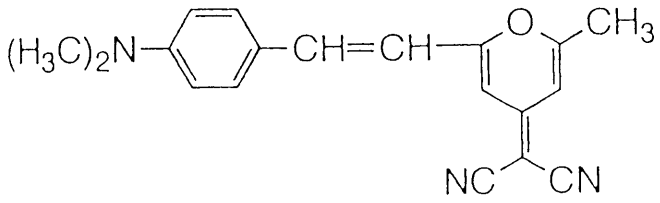

DCM

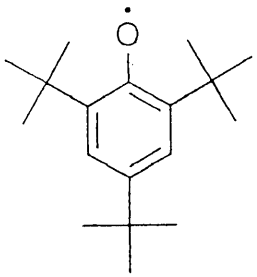

TBPR

(acceptor)

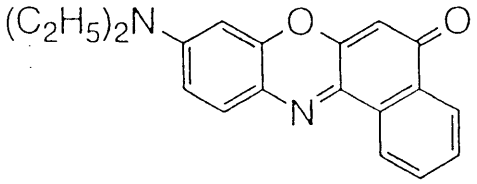

NR

(donor)

CHAPTER 3

RESONANCE ENERGY TRANSFER FROM THE LOWEST EXCITED STATE OF DIPHENYLCARBENE TO DYE MOLECULES: UTILIZATION FOR THE CHARACTERIZATION OF THE TRIPLET-TRIPLET FLUORESCENCE

3.1 Abstract

Triplet-triplet ($T_1 \rightarrow T_0$) fluorescence spectra and decay curves of diphenylcarbene (DPC) in the absence and in the presence of dye molecules such as Rhodamine 6G and Rhodamine B were measured in several organic glasses at 77 K. In the absence of dye molecules, the $T_1 \rightarrow T_0$ fluorescence signals exhibit biexponential decay with the lifetimes of $\sim$30 and $\sim$140 ns, which are attributable to the independent $T_1 \rightarrow T_0$ emission from the individual T_1 sublevels of DPC. In the presence of dye molecules, fluorescence decay signals of both fast and slow components were well analyzed in terms of resonance energy transfer of Förster type from DPC to dye molecule. The reaction scheme of the energy transfer and their various parameters are discussed on the basis of the independent $T_1 \rightarrow T_0$ emission from the individual T_1 sublevels of DPC at low temperature.

3.2 Introduction

Diphenylcarbene (DPC) has been extensively studied over 40 years. In the process, a considerable amount of information about the structure, chemical reactivity, and physical properties of this molecule has been obtained. It is well-known that the fluorescence of DPC is ascribed to the transition from the first excited triplet state (T_1) to the triplet ground state (T_0). Fluorescence spectra of DPC were first reported by Gibbons and Trozzolo[1] and observed in a single crystal[2] and in liquid phase.[3,4] Fluorescence lifetime and quantum yield were also measured for DPC in organic glasses[5] and in liquid phase.[3,4]

Before 1990, it had been considered that fluorescence decay of DPC in low-temperature matrix was composed of only one component and exhibited single-exponential decay. Therefore, fluorescence quantum yield and radiative and nonradiative rate constants of DPC were determined for only one component.[5a] Resonance energy transfer from the excited DPC to fluorescein was also observed and analyzed on the basis of the idea of one component fluorescence.[6] However, Migirdicyan and co-workers found that fluorescence decay curves of DPC and its derivatives in low-temperature Shpol'skii matrix clearly show nonexponential decay and are significantly modified in the presence of a magnetic field,[7] which is similar to the decay of the $T_1 \rightarrow S_0$ phosphorescence of aromatic compounds in a low-temperature matrix.[8]

In this study, it was confirmed that fluorescence decay curves show biexponential with the lifetimes of ~30 and ~140 ns (initial intensity ratio, fast/slow ~0.5) at 77 K. Further, the author attempted to estimate fluorescence quantum yields (ϕ) and radiative (k_r) and nonradiative (k_{nr}) rate constants for the fast and slow components to examine the decay processes quantitatively. Here, he will propose a novel method to estimate these values. Resonance energy transfer of Förster type[9] from the T_1 of DPC to a suitable acceptor molecule gives information about ϕ for each fluorescence components as will be mentioned later. The respective values of k_r and k_{nr} will be obtained from the corresponding ϕ and fluorescence lifetimes. In order to obtain these values, fluorescence decay curves of DPC quenched by the energy transfer to Rhodamine 6G (Rh6G) or Rhodamine B (RhB) were measured. The respective values of ϕ, k_r, and k_{nr} thus estimated will be compared between the fast and slow components and further discussed concerning to the triplet-triplet fluorescence characteristics of DPC at low temperature.

3.3 Experimental Section

3.3.1 Materials.

The precursor of DPC, diphenyldiazomethane, was synthesized by the base-catalyzed oxidation of benzophenone hydrazone (Tokyo Kasei) as described in a previous paper.[10] Rh6G (Tokyo Kasei) and RhB (Nacalai Tesque) were recrystallized from water/methanol mixed solvent. Solvents used in this study are ethanol, EPA (diethyl ether:isopentane:ethanol = 5:5:2), 3-methylpentane (3MP), and 2-methyltetrahydrofuran (MTHF). Spectrograde ethanol (Nacalai Tesque) and Spectrograde diethyl ether (Nacalai Tesque) were used without further purification. Isopentane (Nacalai Tesque) and 3MP (Aldrich) were distilled over $LiAlH_4$. MTHF (Tokyo Kasei), washed with 10 % NaOH and dried over $MgSO_4$, was subjected to fractional distillation over CaH_2 followed by distillation over potassium metal. The sample solutions were degassed by repeated freeze-pump-thaw cycles. The concentration range of diphenyldiazometane was 2×10^{-4} to 2×10^{-3} M.

3.3.2 Measurements.

Photolysis of diphenyldiazometane at 77 K was performed for about 30 seconds with a xenon arc lamp (Ushio, UI-501C) through glass filters (Toshiba UV-29 and Corning 7-54, 300-400 nm). Fluorescence measurements were carried out using a conventional spectrophotometer (Hitachi, 850)

The fluorescence lifetime measurements were carried out with XeCl excimer laser (Lambda Physik 53MSC) pumped dye laser (Lambda Physik FL2002, Coumarin 47, 460 nm, fwhm $\sim$ 6 ns) for excitation pulse. In the case of obtaining time-resolved fluorescence spectra, the second harmonic (320 nm) of dye laser (Rhodamine 101, 640 nm) was used. The fluorescence signals at the wavelength selected by a monochromator (Ritsu MC-20L) were detected by a photomultiplier tube (Hamamatsu, R928). In the presence of dye molecule, a bandpass filter (Corning 5-60) was placed between the sample and the monochromator to prevent strong emission from dye molecule. Signals from the photomultiplier were recorded on a digital storage oscilloscope (Tektronix 2430) interfaced to a personal computer (NEC PC9801).

3.4 Results and Discussion

The UV photolysis of diphenyldiazomethane dispersed in organic glasses at 77 K gives rise to randomly oriented DPC. DPC thus generated gradually reacts with organic solvents even in low-temperature matrix as pointed out by Platz et al.[11] For instance, about 20% of DPC disappears within 30 minutes in ethanol glass at 77 K. However, it was confirmed that the emission from the product is not observed in the wavelength region of the fluorescence of DPC. Therefore, the product does not influence the experimental results.

3.4.1 Steady-State Spectra

Fluorescence (solid) and excitation (broken) spectra of DPC in ethanol glass at 77 K are shown in Figure 1. The fluorescence peak at 480 nm is observed with a shoulder at longer wavelength. This spectrum agrees well with that reported in previous papers.[1,5a] The excitation spectrum consists of two weak bands at 468 and ~415 nm and a strong band at 316 nm. The two bands at 468 (weak) and 316 nm (strong) originate from DPC, which are consistent with those reported in the previous papers,[1,5a] whereas the band at ~415 nm is likely from impurities. Spectral features of both fluorescence and excitation spectra in other organic glasses (EPA, 3MP, and MTHF) are quite similar to those in the ethanol one. The peak positions of these spectra are listed in Table 1. The peak positions of fluorescence spectra are

observed nearly at 480 nm while those of excitation spectra are at 468 (weak) and ~318 nm (strong) in these glasses. This result indicates that electronic spectra of DPC are not influenced by properties of the medium (e.g., solvent polarity or viscosity).

According to the electronic spectra of DPC trapped in substitutional sites of a benzophenone single crystal,[2] a sharp zero-phonon line (470.7 nm) is observed with a broad sideband extending to high energy in absorption (λ_{max} ~ 465 nm) and to low energy in emission (λ_{max} ~ 476 nm) in the temperature range 2 - 20 K. The sharp zero-phonon line disappears with increasing temperature while the broad sideband is observed still above 20 K. The fluorescence and excitation spectra observed in this study closely resemble these broad sidebands. The geometry of DPC in the benzophenone single crystal was determined to be nonplanar with a central C-C-C angle of 140° and dihedral angles of 29.9° and 26.7° by means of electron nuclear double resonance (ENDOR) spectroscopy.[12] It is therefore suggested that the fluorescence band observed in this study is from the nonplanar geometry similar to DPC in the benzophenone single crystal.

On the other hand, Figure 1 also shows absorption spectra of Rh6G (dotted) and RhB (dashed). The spectral overlaps between the fluorescence of DPC and the absorption of dye molecules are significant. Since resonance energy transfer efficiency from DPC to dye molecule increases with increasing spectral overlap,[9] this type of energy transfer from DPC to dye molecule is expected

to occur.

3.4.2 Fluorescence Decays.

Fluorescence decay curve of DPC (A) in ethanol glass at 77 K is displayed on semilogarithmic scale in Figure 2. The solid curve (B) shows a calculated decay curve of single exponential of 115 ns. Obviously the decay curve (A) is nonexponential. The decay curve (A) is analyzed as a sum of two exponential decays with the lifetimes of 25 and 115 ns and with the corresponding initial intensities of 0.30 and 0.70, respectively. The plot of the weighted residuals clearly shows that this biexponential analysis is valid. In other organic glasses at 77 K, fluorescence decay curves of DPC are also analyzed as biexponential decay. The lifetimes of the two components, the corresponding initial intensity, and the ratio of initial intensity (A_1/A_2) are summarized in Table 2. On the other hand, time-resolved fluorescence spectra in the organic glasses at 77 K remain unchanged as the time proceeds and agree well with steady state fluorescence spectrum.

As a result, three characteristic features are found in the fluorescence decays of DPC regardless of the properties of the glasses: (a) The lifetimes of the fast component and the slow one are $\sim$30 ns and $\sim$140 ns (115 ns in ethanol), respectively. (b) The initial intensity ratio of two components (A_1/A_2) is $\sim$0.5. (c) Time-resolved fluorescence spectra almost remain unchanged as

the time proceeds.

The nonexponential fluorescence decay of DPC in low-temperature matrix was also observed by Migirdicyan and co-workers.[7] They have explained this result as follows: the independent fluorescence ($T_{1x} \rightarrow T_{0x}$, $T_{1y} \rightarrow T_{0y}$, and $T_{1z} \rightarrow T_{0z}$) are emitted from the individual T_{1u} (u = x, y, z) sublevels at a rate faster than the spin-lattice relaxation between the different sublevels. The depopulation rate of the isolated T_{1u} sublevels should be equal in the absence of spin-orbit interaction and nonradiative decay processes. However, the wave functions describing the T_{1u} sublevels are mixed with those of singlet states possessing the same symmetry by spin-orbit coupling. Consequently, the fluorescence decay of DPC is composed of three components with distinct depopulation rates caused by different intersystem crossing rates from the T_{1u} sublevels.

The experimental results can be also explained by the idea of the independent emission from the individual T_1 sublevels of DPC. That is, the fast component is composed of the emission from only a specific sublevel of T_1 whose depopulation rate is faster than the others, while the slow component is composed of those from two other sublevels. According to this interpretation, the initial intensity ratio (A_1/A_2) reflects the population of the corresponding sublevels in the ground state, T_0. Since the zero-field splitting energy of T_0 (D/hc = 0.405 cm^{-1} and E/hc = 0.019 cm^{-1} in the benzophenone single crystal[13]) is much smaller than the energy of kT (53.4 cm^{-1}) at 77 K, the populations of the

three T_{0u} sublevels are equal. Consequently, the initial intensity ratio (A_1/A_2) may be close to 0.5. The sublevels of both T_0 and T_1 are almost degenerate so that the observation (c) is due to the same transition energy of the three $T_{1u} \rightarrow T_{0u}$ transitions.

3.4.3 Estimated Values of Fluorescence Quantum Yields and Radiative and Nonradiative Rate Constants for the Fast and Slow Components

The author proposes a novel method to estimate the values of fluorescence quantum yields and radiative and nonradiative rate constants for the fast and slow components of DPC in ethanol glass at 77 K. The method is to use the resonance energy transfer from the excited DPC to a suitable acceptor molecule. In general, one needs to measure the fluorescence lifetime and quantum yield to determine the radiative and nonradiative rate constants experimentally. In the case of this study, however, the fluorescence quantum yields for the fast and slow components of DPC cannot be measured independently by means of a conventional method using a standard such as quinine bisulfate in aqueous H_2SO_4 solution.

According to Förster theory,[9] the critical transfer distance (R_0) of resonance energy transfer can be expressed by

$$R_0^6 = \frac{9000(\ln 10)\,\kappa^2\,\phi}{128\,\pi^5 n^4 N}\,J \qquad (1)$$

where κ^2 and ϕ are the orientation factor and fluorescence quantum yield of the donor in the absence of energy transfer, respectively; n and N are refractive index of the medium and Avogadro's number, respectively. J is the spectral overlap integral as expressed as follows:

$$J = \int \frac{F_D(\tilde{\nu})\,\varepsilon_A(\tilde{\nu})}{\tilde{\nu}^4}\,d\tilde{\nu} \qquad (2)$$

where $F_D(\tilde{\nu})$ and $\varepsilon_A(\tilde{\nu})$ are the spectra of donor emission normalized to unity and the molar extinction coefficient of acceptor, respectively. Accordingly, the values of ϕ for each fluorescence component can be estimated from the corresponding values of R_0. In order to determine the values of R_0 for both fluorescence components simultaneously, the fluorescence decay curves quenched by Rh6G or RhB were measured.

Fluorescence decay curves of DPC in the presence of Rh6G or RhB in ethanol glass at 77 K are shown in Figures 3 and 4, respectively. The fluorescence intensities are normalized at the time origin. The apparent fluorescence lifetime decreases with increasing concentration of dye molecule. It is confirmed that the T_1 state of DPC is efficiently quenched by Rh6G or RhB. Wu and Trozzolo observed resonance energy transfer from DPC to fluorescein by means of fluorescence decay measurement and determined the value of R_0 to be 6.1 nm^6. The author used Rh6G or RhB as the energy acceptor instead of fluorescein, because a considerable amount of emission from fluorescein mixes into the

fluorescence of DPC. This emission prevents analyzing the quenched decay curves of DPC strictly.

The fluorescence decay of the donor undergoing dipole-dipole resonance energy transfer in uniformly distributed and randomly oriented system is expressed as follows:[14]

$$I(t) = A \exp[-t/\tau - X(t/\tau)^{1/2}] \quad (3)$$

where τ is the fluorescence lifetime of donor in the absence of acceptor and

$$X = g(3/4000)\pi^{3/2} N R_0^3 C_A \quad (4)$$

in which g is the orientation factor, C_A is the concentration of acceptor, N and R_0 are denoted in eq. 1. In the case of this study, the fluorescence of DPC contains two components so that the fluorescence decay of DPC in the presence of dye molecule is expressed by

$$I(t) = \sum Ai \exp[-t/\tau_i - Xi(t/\tau_i)^{1/2}] \quad (i = 1, 2) \quad (5)$$

where τ_i and Xi are the fluorescence lifetime and X for each fluorescence component of DPC, and i = 1 and 2 represent the fast fluorescence component and the slow one, respectively.

The value of R_0 for the fast and slow components can be obtained by determining X_1 and X_2 by means of curve fitting procedure at several concentrations of dye molecule. The convolution and subsequent nonlinear least-squares method were carried out with the parameters (X_1 and X_2) and the fixed constant values (A_1 = 0.3, A_2 = 0.7, τ_1 = 25 ns and τ_2 = 115 ns) which determined from the absence of dye molecule. A calculated decay curve (solid) with the parameters (X_1 = 0.70 and

X_2 = 1.57) and an observed decay curve in the presence of 4 mM Rh6G are shown in Figure 5. The plot of the weighted residuals clearly indicates that the two curves fit very well. Other fluorescence decay curves in the presence of dye molecule were fitted in the same manner.

The plots of $X1$ (□, △) and $X2$ (■, ▲) vs concentration of dye molecule are shown in Figure 6. Both X_1 and X_2 increase linearly with increasing concentration of dye molecules as predicted from eq. 4. The values of R_{01} and R_{02} are calculated from the slope of the plot, $g(3/4000)\,\pi^{3/2}NR_0^3$, where g for a rigid random orientation is 0.845.[15] The values of R_{01} and R_{02} for DPC/Rh6G combination are 3.6 and 4.7 nm, and those for DPC/RhB combination are 3.5 and 4.5 nm, respectively. Comparing the values of R_{0i} between DPC/Rh6G and DPC/RhB, the values of R_{0i} for DPC/Rh6G are slightly larger than those for DPC/RhB for both the fast and slow components. This result is consistent with the prediction from the spectral overlap J, in which the value of DPC/Rh6G (25×10^{-14} cm^6) is larger than that of DPC/RhB (19×10^{-14} cm^6).

The value of ϕ_i for the fast and slow components can be estimated from the Förster equation (1), where the respective values of R_{01} and R_{02} are substituted into the Förster equation (1). It should be emphasized that the values of J for both fluorescence components are equal because time-resolved fluorescence spectra remain unchanged as the time proceeds. The

value $\kappa^2 = 0.476$ is quoted for a rigid random orientation.[15] The value of n for ethanol at 77 K has not been reported so far; therefore, we determined this value as 1.45 using $n = 1.37$ at 273 K and its temperature dependence $dn/dT = 4 \times 10^{-4}$ K^{-1}.[16] Consequently, the calculated values of ϕ_1 and ϕ_2 are 0.09 and 0.46 for DPC/Rh6G combination, and 0.11 and 0.47 for DPC/RhB combination, respectively. Comparing the values of ϕ_i between DPC/Rh6G and DPC/RhB, these values agree well with each other. Thus the similar values of ϕ_i are obtained from two different DPC/dye combinations. These values are listed in Table 3. The average values of ϕ_1 and ϕ_2 are about 0.1 and 0.5, respectively.

Considering the total fluorescence quantum yield (ϕ_{tot}), this is expressed as follows:

$$\phi_{tot} = A_1 \phi_1 + A_2 \phi_2 \quad (A_1 + A_2 = 1),$$

where A_1 and A_2 are the fractions of the initial intensities denoted in eq. 5. The value of ϕ_{tot} is estimated to be ~ 0.4. Taking account of the uncertainty of the value of n at 77 K and experimental errors, this value is in reasonable agreement with the experimental value (0.2) in ethanol glass at 77 K reported by Ono and Ware.[5a] Therefore, the values of both ϕ_1 and ϕ_2 obtained from energy transfer analysis are reliable.

The respective values of k_{ri} and k_{nri} for the fast and slow components can be easily calculated from the relation of $k_{ri} = \phi_i / \tau_i$ and $k_{nri} = (1-\phi_i)/\tau_i$ ($i = 1, 2$). The values of k_{ri} and K_{nri} ($i = 1, 2$) are summarized in Table 3.

It is obvious that the values of k_{ri} for both the fast and slow components are nearly equal (4×10^6 s^{-1}) for both DPC/dye combinations. This result clearly indicates that the radiative processes from the individual T_1 sublevels are not influenced by some kinds of interaction such as spin-orbit coupling. Since the radiative processes of the individual transitions ($T_{1x} \rightarrow T_{0x}$, $T_{1y} \rightarrow T_{0y}$, and $T_{1z} \rightarrow T_{0z}$) of DPC are electronically allowed, the corresponding transition moments are not so perturbed.

On the other hand, the value of nonradiative rate constant for the fast component ($k_{nr1} \sim 36 \times 10^6$ s^{-1}) is about 7-8 times as much as that for the slow one ($k_{nr2} \sim 5 \times 10^6$ s^{-1}). The biexponential fluorescence decays of DPC in some organic glasses at 77 K are definitely caused by this difference between k_{nr1} and k_{nr2}. This difference is ascribed to the distinct intersystem crossing rates from the corresponding sublevels of T_1 to lower energy singlet states (S_n) as reported by Migirdicyan and co-workers.[7] In particular, it is probably suggested that there is a specific spin sublevel in T_1 which strongly couples to lower S_n by spin-orbit interaction. Migirdicyan and co-workers have also presented that three or four singlet states exist between T_0 and T_1 of DPC from a molecular orbital calculation (CS-INDO CI method).[7c]

Here, let us consider the reason why fluorescence decay curves of DPC in some organic glasses at 77 K exhibit biexponential with the initial intensity ratio, $A_1/A_2 \sim 0.5$. Two

possible explanations might be offered to account for the reason; (1) Spin-orbit coupling interact only a specific spin sublevel but not two others of T_1. (2) Even if the three intersystem crossing rates are different, the depopulation rates of two spin sublevels of T_1 except for that of the specific one are equalized by the spin-lattice relaxation process between the two sublevels because it still remains a question whether spin-lattice relaxation can sufficiently be suppressed at 77 K. At the present stage, it is impossible to decide which explanation is proper.

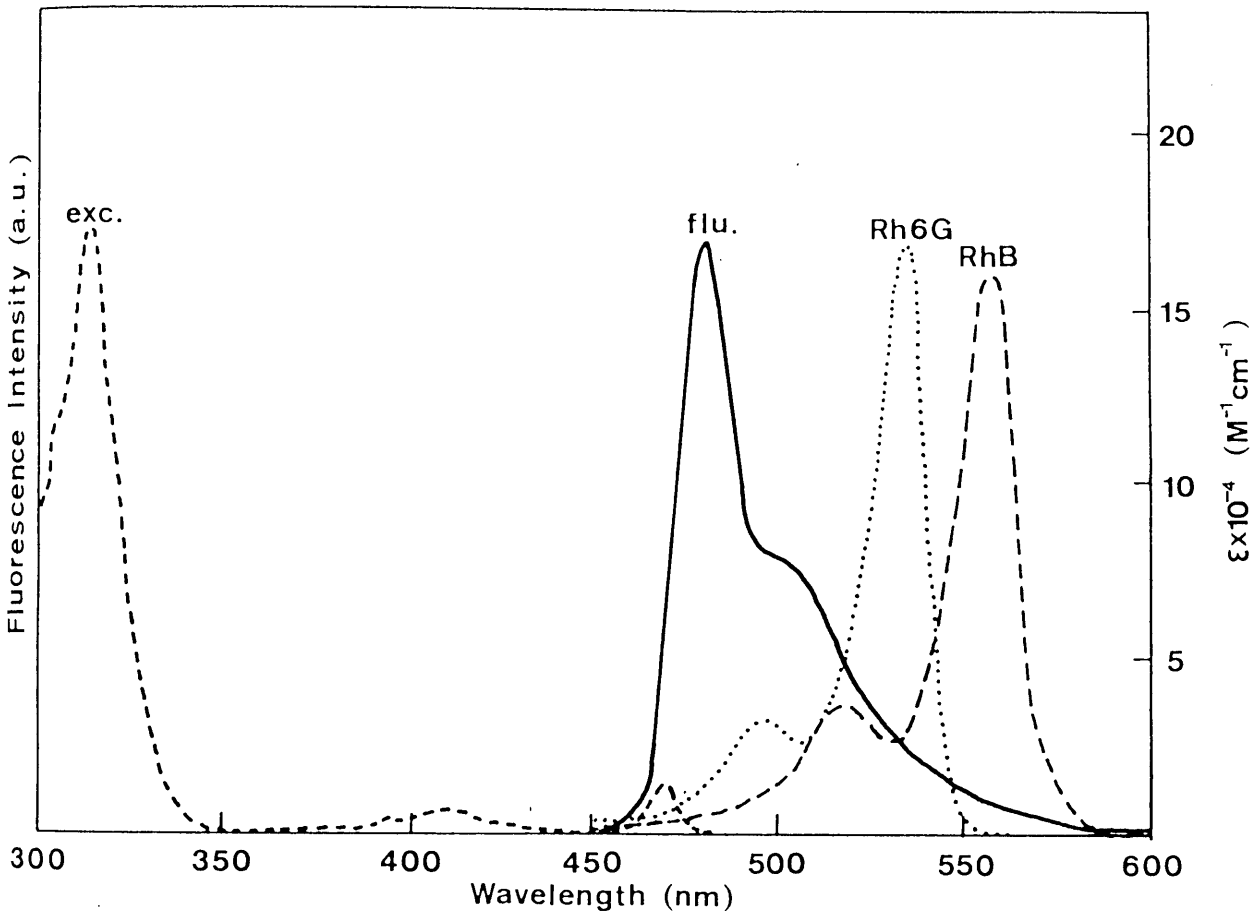

Figure 1. Fluorescence (solid) and excitation (broken) spectra of diphenylcarbene and absorption spectra of Rhodamine 6G (Rh6G) and Rhodamine B (RhB) in ethanol glass at 77 K.

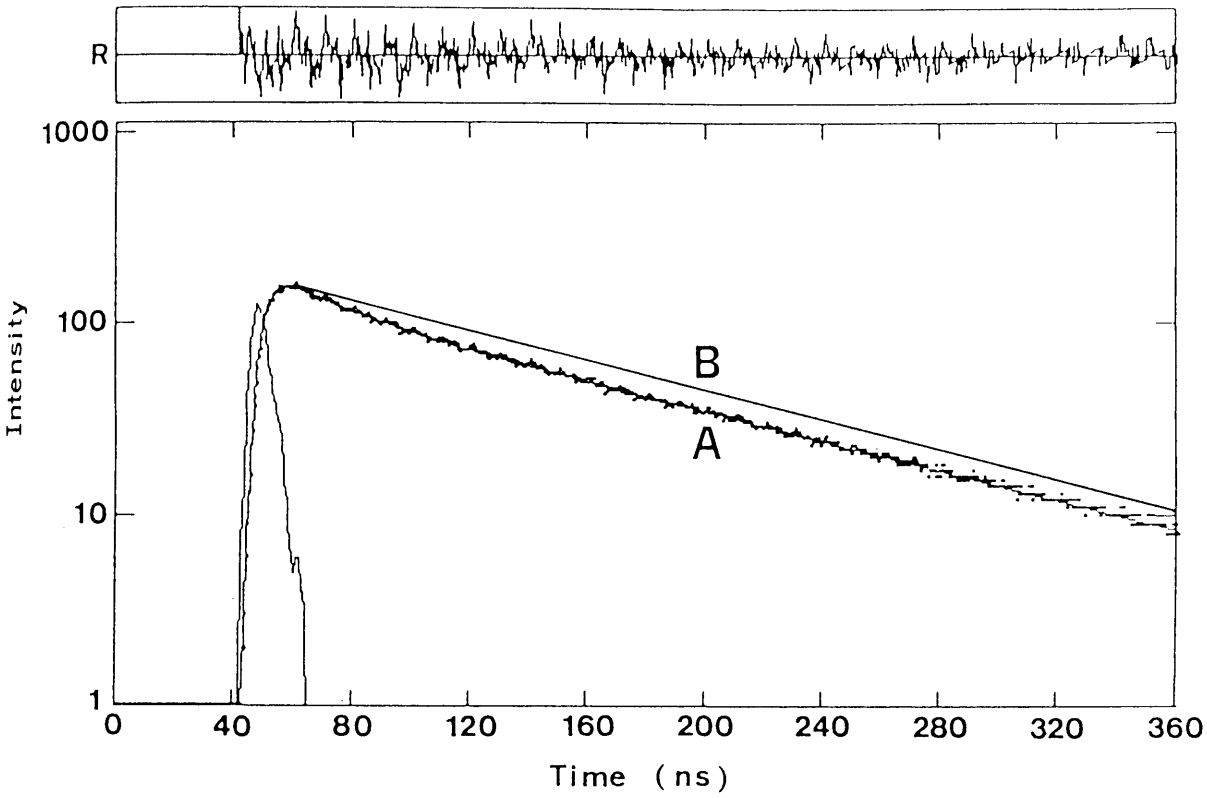

Figure 2. Fluorescence decay curve of diphenylcarbene (A) in ethanol glass at 77 K. The solid curve (B) is a calculated decay curve of single exponential (115 ns). The weighted residuals show the best fitting with the lifetimes of 25 and 115 ns and with corresponding initial intensities of 0.30 and 0.70.

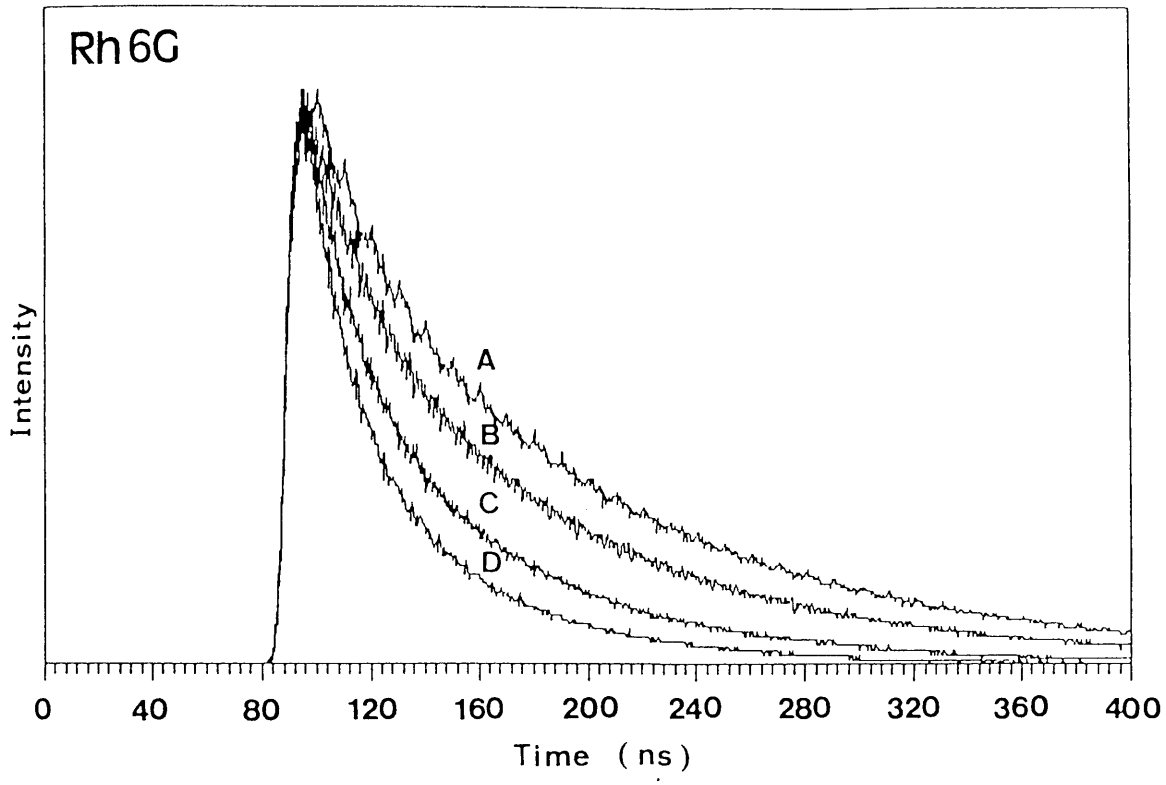

Figure 3. Fluorescence decay curves of diphenylcarbene with (A) 0, (B) 1, (C) 3, and (D) 5 mM Rhodamine 6G in ethanol glass at 77 K.

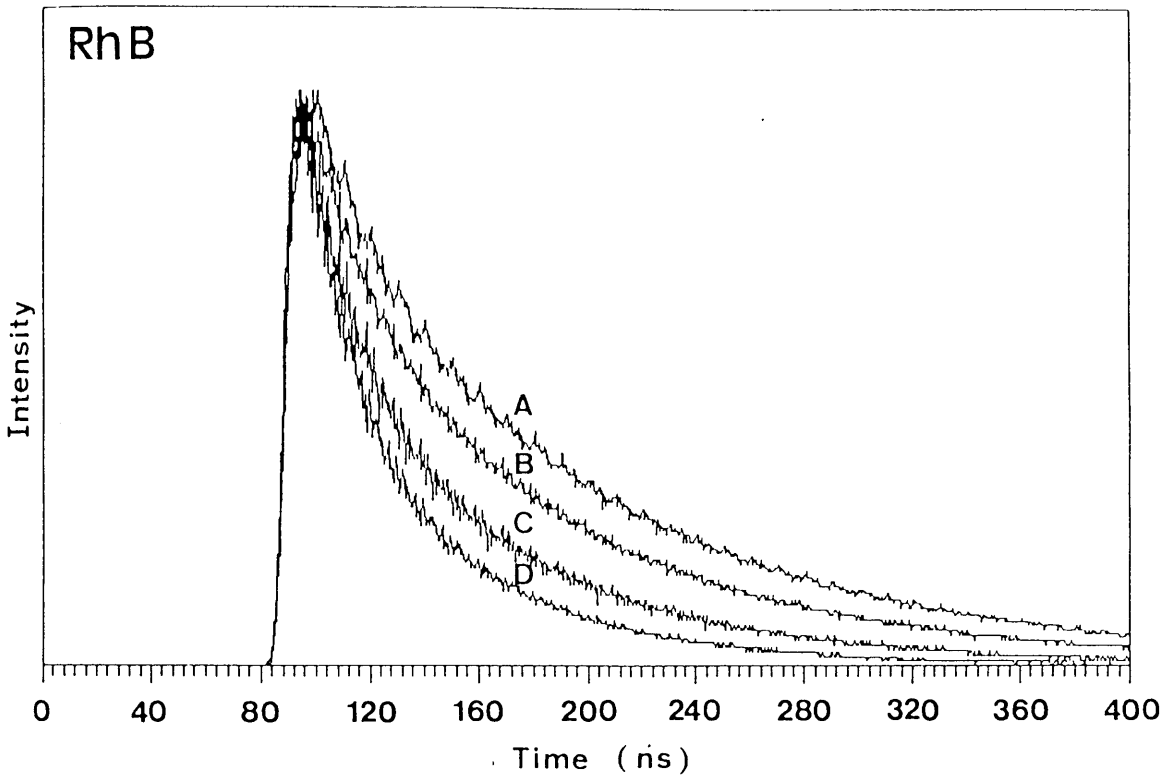

Figure 4. Fluorescence decay curves of diphenylcarbene with (A) 0, (B) 1, (C) 3, and (D) 5 mM Rhodamine B in ethanol glass at 77 K.

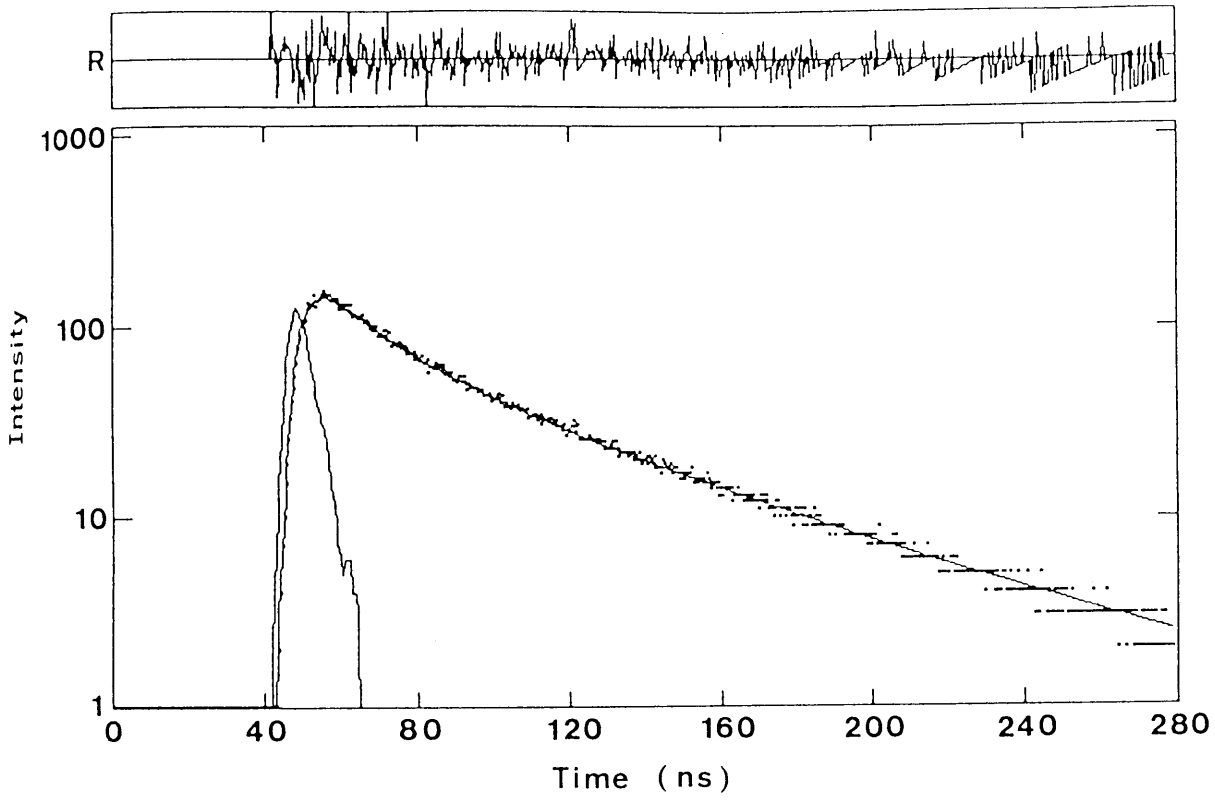

Figure 5. Fluorescence decay curve of diphenylcarbene with 4 mM Rhodamine 6G in ethanol glass at 77 K. The solid curve was calculated from eq. 5 by using the values A_1 = 0.3, A_2 = 0.7, τ_1 = 25 ns, τ_2= 115 ns, X1 = 0.70, and X2 = 1.57.

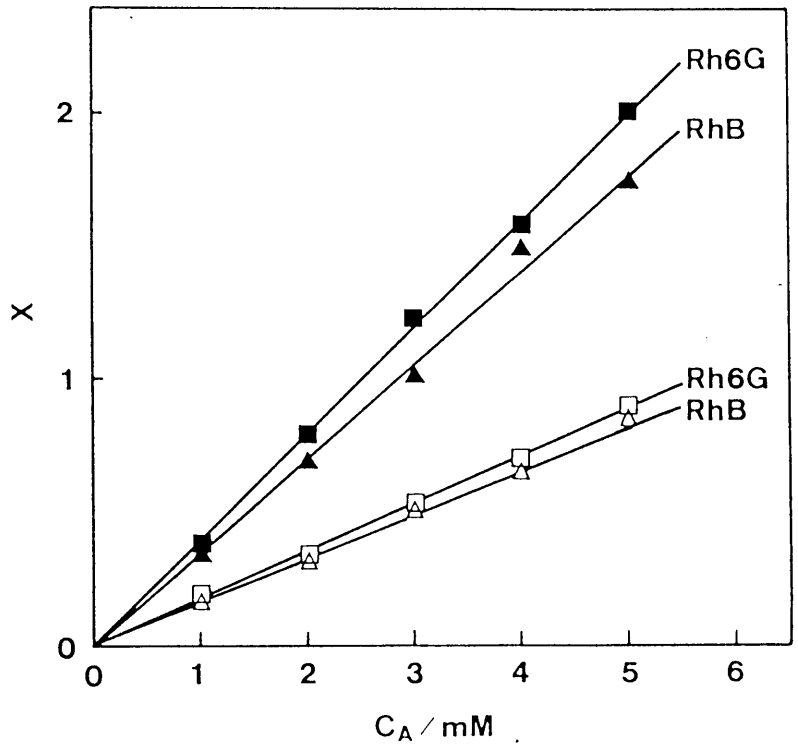

Figure 6. Plots of X_1 (□ , △) and X_2 (■ , ▲) vs concentration of dye molecules.

TABLE 1. Peak Position of Fluorescence and Excitation Spectra in Organic Glasses at 77 K

glass	fluorescence	excitation[a]	
	λ_{max}/nm	λ (weak)/nm	λ (strong)/nm
EtOH	480	468	316
EPA	479	468	318
MTHF	477	468	320
3MP	482	468	317

[a] Excitation spectra are uncorrected.

TABLE 2. Fluorescence Lifetimes (τ_i), Initial Intensity[a] (Ai), and Initial Intensity Ratio (A_1/A_2) in Organic Glasses at 77 K

glass	fast component		slow component		A_1/A_2
	A_1	τ_1/ns	A_2	τ_2/ns	
EtOH	0.30	25	0.70	115	0.43
EPA	0.31	29	0.69	146	0.45
MTHF	0.28	32	0.72	141	0.39
3MP	0.34	25	0.66	141	0.52

[a] Initial intensity are normalized: $A_1 + A_2 = 1$.

TABLE 3. Estimated Values of Fluorescence Quantum Yields (ϕ_i), Radiative Rate Constant[a] (k_{ri}), and Nonradiative Rate Constant[b] (k_{nri}) in Ethanol Glass at 77K (i = 1, 2)

acceptor	fast component			slow component		
	ϕ_1	$k_{r1}/10^6 s^{-1}$	$k_{nr1}/10^6 s^{-1}$	ϕ_2	$k_{r2}/10^6 s^{-1}$	$k_{nr2}/10^6 s^{-1}$
Rh6G	0.09	3.7	36	0.46	4.0	4.7
RhB	0.11	4.3	36	0.47	4.2	4.5

[a] $k_{ri} = \phi_i / \tau_i$, τ_i is fluorescence lifetime for each component.

[b] $k_{nri} = (1-\phi_i)/\tau_i$

References

(1) (a) Gibbons, W. A.;Trozzolo, A. M. *J. Am. Chem. Soc.* 1966, *88*, 172.

(b) Trozzolo, M. A.;Gibbons, W. A. *J. Am. Chem. Soc.* 1967, *89*, 239.

(2) Anderson, R. J.;Kohler, B. E.;Stevenson, J. M. *J. Chem. Phys.* 1979, *71*, 1559.

(3) (a) Scaiano, J. C.;Weir, D. *Chem. Phys. Lett.* 1987, *141*,503.

(b) Scaiano, J. C.;Weir, D. *Can. J. Chem.* 1988, *66*, 491.

(4) Fujiwara, Y.;Sasaki, M.;Tanimoto, Y.;Itoh, M. *J. Phys. Chem.* 1989, *93*, 702.

(5) (a) Ono, Y.;Ware, W. R. *J. Phys. Chem.* 1983, *87*, 4426.

(b) Ware, W. R.;Sullivan, P. J. *J. Chem. Phys.* 1968, *49*, 1445.

(6) Wu, K. C.;Trozzolo, A. M. *J. Phys. Chem.* 1978, *82*, 1827.

(7)(a) Haider, K. W.;Platz, M. S.;Despres, A.; Lejeune, V.; Migirdicyan, E. *J. Phys. Chem.* 1990, *94*, 142. (b) Despres, A.;Lejeune, V.;Migirdicyan, E.;Platz, M. S. *J. Phys. Chem.* 1992, *96*, 2486. (c) Despres, A.;Lejeune, V.;Migirdicyan, E.;Admasu, A.;Platz, M. S.; Berthier, G.; Parisel, O.; Flament, J. P.; Baraldi, I.; Momicchioli, F. *J. Phys. Chem.* 1993, *97*, 13358.

(d) Kozankiewicz, B.;Despres, A.;Lejeune, V.;Migirdicyan, E.; Olson, D.; Michalak, J.;Platz, M. S. *J. Phys. Chem.* 1994, *98*, 10419.

(8) (a) De Groot, M. S.;Hesselmann, I. A. M.;Van der Waals, J. H.

Mol. Phys. 1967, *12*, 259.

(b) Hall, L.;Armstrong, A.;Moomaw, W.;El-Sayed, M. A. *J. Chem. Phys.* 1968, *48*, 1395.

(9) Förster, T. *Discussions Faraday Soc.* 1959, *27*, 7.

(10) Tanimoto, Y.;Nagano, M.;Fujuwara, Y.;Kohtani, S.;Itoh, M. *J. Photochem. Photobiol. A: Chem.* 1993, *74*, 153.

(11) Platz, M. S.;Senthilnathan, V. P.;Wright, B. B.; McCurdy Jr., C. W. *J. Am. Chem. Soc.* 1982, *104*, 6494.

(12) Anderson, R. J. M.;Kohler, B. E. *J. Chem. Phys.* 1976, *65*, 2451.

(13) Brandon, R. W.;Closs, G. L.;Davoust, C. E.;Hutchison Jr., C. A.;Kohler, B. E.;Silbey, R. *J. Chem. Phys.* 1965, *43*, 2006.

(14) Lamola, A. A.;Turro, N. J. *Energy transfer and organic photochemistry*; Wiley-Interscience, New York, 1969; p41

(15) Eisenthal, K. B.;Siegel, S. *J. Chem. Phys.* 1964, *41*, 652.

(16) Smith, T. E.;Bonner, R. F. *Anal. Chem.* 1952, *3*, 517.

APPENDIX

Intersystem crossing rate constant, k_{isc}, can be described by the golden rule expression[1]

$$k_{isc} = (2\pi/h)|V|^2 F \rho$$

where F is the Frank-Condon factor governed by the vibrational overlap between the initial and final states and ρ is the density of final states. V is an electronic matrix element describing the spin-orbit coupling between the singlet and triplet state, which is expressed as follows:

$$\langle \Phi_s \sigma | H_{so} | \Phi_t T_u \rangle \quad (u = x, y \text{ and } z),$$

where H_{so} is the Hamiltonian for spin-orbit coupling. Φ_s and Φ_t are spatial wavefunctions of singlet and triplet states, respectively. σ is the singlet spin function and T_u are the triplet spin functions which the total spin anglar momentum are oriented in the principal planes u = 0.[2]

The selection rule of intersystem crossing process is determined whether V is vanishing or not. If V is non-vanishing, the intersystem crossing can take place. According to group theory, non-vanishing matrix element is achieved when the total wavefunctions of singlet and triplet states belong to the same irreducible representation.[2] In the case of the planar C_{2v} diphenylcarbene, the energy levels and the total symmetry of all singlet and triplet states are predicted by a molecular orbital calculation (CS-INDO CI method)[3] as shown in figure A. Among the three components of the lowest excited triplet state (T_1), T_z sublevel can couple with S_2 and S_3 singlets having the same total

symmetry A_1 and T_x sublevel can mix with S_1 singlet with the total symmetry B_1, whereas T_y sublevel cannot mix with singlet states. As a consequent, the rates of intersystem crossing from each individual T_1 sublevel to singlet states would be different, which leads to nonexponential fluorescence decays.

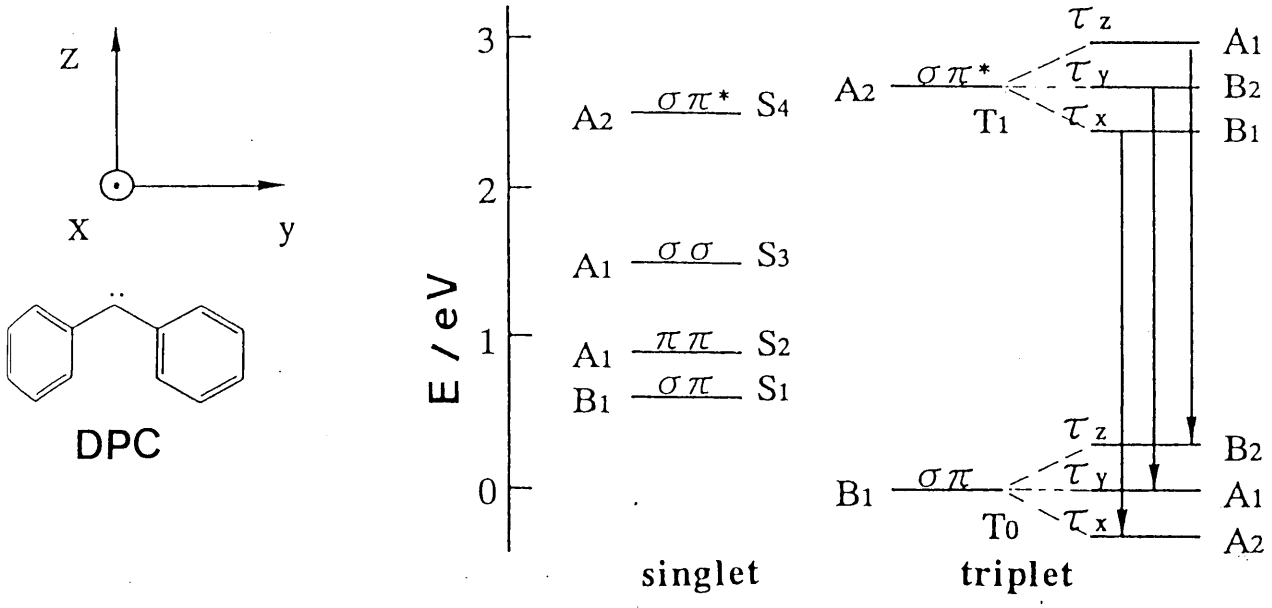

Figure A. Energy level diagram of the planar diphenylcarbene (Taken from reference 3)

References

(1) Atkins, P. W. *Molecular Quantum Mechanics*, Oxford, New York, 1983; p 198.

(2) McGlynn, S. P.; Azumi T.; Kinoshita M. *The Triplet State*, Prentice-Hall, Englewood Cliffs, 1969.

(3) Despres, A.;Lejeune, V.;Migirdicyan, E.;Admasu, A.;Platz, M. S.; Berthier, G.; Parisel, O.; Flament, J. P.; Baraldi, I.; Momicchioli, F. *J. Phys. Chem.* 1993, *97*, 13358.

LIST OF COMPOUNDS

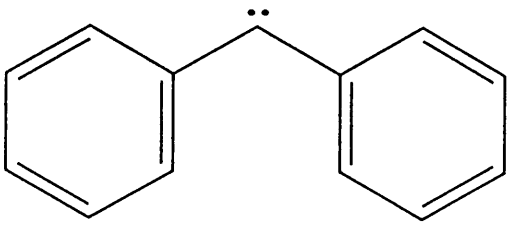

diphenylcarbene (DPC)

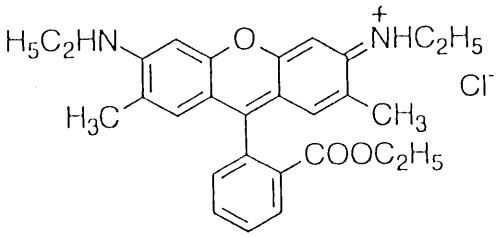

RHODAMINE 6G

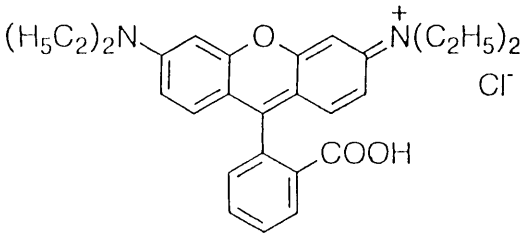

RHODAMINE B

CHAPTER 4

LASER FLASH PHOTOLYSIS STUDY OF THE PRIMARY PROCESS IN 1,8-BIS[4-(α -DIAZOBENZOYL)PHENOXY]OCTANE: EFFECTS OF LASER AND MAGNETIC FIELD

4.1 Abstract

Upon the 308 nm laser pulse excitation of 1,8-bis[4-(α-diazobenzoyl)phenoxy]octane in benzene, transient absorption bands due to the chromophores of the diphenylcarbene and the diphenylmethyl radical appear in the 320-480 nm region. Intensity ratio of the former to the latter decreases with increasing the laser power. The external magnetic field effect (0.6 T) is observed on the decay curve of the methyl radical *only* under the intense laser excitation. All the observations are interpreted in terms of the reaction scheme proposed.

4.2 Introduction

Many efforts to control organic photoreaction by intense laser pulses have been carried out after the pioneering work by Turro's group.[1,2] With the aid of high intensity laser pulses, reaction intermediates like excited states and radicals are generated in high concentration and are also excited within a single pulse. Thus reactions between short-lived intermediates and those from their excited states take place, which can not be achievable by a conventional lamp. Recently, in the preparative laser photolysis study of a bichromophoric compound, 1,2-bis[2-(α -diazobenzoyl) phenyl]ethane, Hannemann and Wirz reported the formation of a new compound by photolyzing two diazo groups in it.[3] On the other hand, magnetic field effect (MFE) on the photoreaction of bichromophoric chain molecules has been extensively studied.[4-7] It is because the chain-linked biradicals generated by the end-to-end photoreaction exhibit significant MFE, and therefore are highly suitable for the precise understanding of its mechanism.

This chapter deals with the laser flash photolysis study of the laser and magnetic field effects on the primary process of a bichromophoric chain-linked bisdiazo compound.

4.3 Experimental Section

4.3.1 Materials

1,8-Bis[4-(benzoyl)phenoxy]octane. A mixture of 4-hydroxybenzophenone (2.5 g) and potassium carbonate (2.07 g) in dry dimethylformamide (DMF, 7.5 ml) was stirred at 50 ℃ for 20 h. To the mixture was added slowly 1,8-dibromooctane (1.36 g) in dry DMF (5 ml) and stirred at 100 ℃ for 8h. The reaction mixture was treated with 10% aqueous sodium hydroxide and water, and recrystallized from benzene-ethanol, yielding white crystals (1.93 g). m.p. 141-142 ℃; ^{1}H NMR($CDCl_3$) δ 1.2-2.0 (12H, br, $-CH_2-$), 3.97 (4H, t, J=6.3 Hz, $-OCH_2-$), 6.9-7.4 (18H, m, Ar-H); IR (KBr) 1640 (>C=O), 2870, 2950 ($-CH_2-$) cm^{-1}; MS, m/e 506(M^+); Anal. Calcd. for $C_{34}H_{34}O_4$: C, 80.60; H, 6.76. Found: C, 80.65; H, 6.76.

1,8-Bis[4-(benzoyl)phenoxy]octane dihydrazone. The mixture of the bisketone(1.0 g) and hydrazine hydrate (4.0 g) in benzene(10 ml)-ethanol (8 ml) was heated under reflux for 70 h. Hydrazine hydrate (3.0 g) was further added to the solution and it was refluxed for 20 h to complete the reaction. The solvent was evaporated, and the residue was recrystallized from benzene-ethanol, yielding white crystals (0.49 g). m.p. 120-122 ℃; ^{1}H NMR($CDCl_3$) δ 1.2-2.0 (12H, br, $-CH_2-$), 3.98 (4H, t, J=6.3 Hz, $-OCH_2-$), 5.0-5.6 (4H, br, $=N-NH_2$), 6.9-7.4 (18H, m, Ar-H); IR(KBr) 1650 ($-NH_2$), 2870, 2950 ($-CH_2-$), 3390 ($-NH_2$) cm^{-1}; MS, m/e 534 (M^+); Anal. Calcd. for $C_{34}H_{38}N_4O_2$: C, 76.40; H, 7.12; N,

10.49. Found: C, 76.62; H, 7.07; N, 10.37.

1,8-Bis[4-(α-diazobenzoyl)phenoxy]octane (BDO). To a stirred solution of the bishydrazone (0.34 g) in dry tetrahydrofuran (100ml) were added active manganese dioxide (Merck, 5953 activated granular, 3.0 g) and a few drops of saturated ethanolic potassium hydroxide in the dark. The reaction was monitored by measuring the growth of either the IR absorption at 2030 cm^{-1} or the visible one at 534 nm due to the diazo group of the aliquots. The absorption becomes maximum at 7 h, when the mixture was filtered. The red-wine solution was concentrated to 50 ml under reduced pressure and cooled to -20 ℃, yielding purple crystals (0.09 g). m.p. 130-134 ℃ dec; ^1H NMR($CDCl_3$) δ 1.2-2.0 (12H, br, $-CH_2-$), 3.97 (4H, t, J=6.3 Hz, $-OCH_2-$), 6.9-7.4 (18H, m, Ar-H); IR(KBr) 2030 ($>C=N_2$), 2870, 2950 ($-CH_2-$); MS, m/e 502($(M - N_2)^+$), 474($(M - 2N_2)^+$); Anal. Calcd. for $C_{34}H_{34}N_4O_2$: C, 76.95; H, 6.46; N, 10.56. Found: C, 76.65; H, 6.59; N, 10.25.

1-[4-(α-diazobenzoyl)phenoxy]octane (DO). DO was prepared, purified and characterized following a similar procedure to that of BDO. m.p. 51 ℃ dec; ^1H NMR($CDCl_3$) δ 0.89 (3H, t, J=6.2, $-CH_3$), 1.2-2.0 (12H, br, $-CH_2-$), 3.97 (2H, t, J=6.3 Hz, $-OCH_2-$), 6.9-7.4 (9H, m, Ar-H); IR(KBr) 2030($>C=N_2$), 2870, 2950 ($-CH_2-$) cm^{-1}; MS, m/e 294 (M^+); Anal Calcd. for $C_{21}H_{26}N_2O_1$ C, 78.22, H, 8.13, N, 8.69. Found: C, 78.37; H, 8.24; N, 8.11.

In spectroscopic measurements, spectro-grade benzene was used as supplied. 2-Methyltetrahydrofuran was distilled over potassium metal. Sample solution was degassed by the repeated freeze-pump-

thaw cycles.

4.3.2 Instruments and methods

Steady-state photolysis was carried out using a xenon arc lamp (Ushio, UXL-500-O) equipped with glass filters (Sigma Koki, UTVAF-50S-33U and UTF-50S-30U)(λ = 300-400 nm) as an exciting light source. UV absorption measurements at 77 K was carried out using a conventional spectrophotometer (Hitachi, U-3200).

Laser flash photolysis was carried out using a XeCl excimer laser (Lumonics 500, 308 nm, 80 mJ/pulse, pulse width 8-12 ns) as an exciting light source. Laser power was estimated roughly from its specifications and varied using neutral density filters. The details of the apparatus is shown in Figure 1.

4.4 Results and discussion

4.4.1 Steady-state photolysis at 77 K

Figure 2 shows the UV absorption spectra of BDO in 2-methyltetrahydrofuran rigid glass at 77 K. Upon photoirradiation of BDO, a new absorption band peaked at around 320 nm appears with the concomitant decrease in the intensity of absorption band of BDO peaked at around 290 nm. Since it disappears after warming up to room temperature, the new band is attributable to unstable intermediates. From the analogy of its absorption and fluorescence (λ_{max}=496 nm, not shown in Figure 2) spectra with those of diphenylcarbene,[8] the absorption spectrum peaked at 320 nm is attributable to that of the diphenylcarbene group of the reaction intermediates generated from BDO.

4.4.2 Laser flash photolysis

Effect of laser intensity: Figure 3 shows the transient absorption spectra of a deaerated benzene solution of BDO under two laser fluence. When a deaerated benzene solution of BDO is excited by a weak laser pulse (308 nm, ca. 30 mJ/cm^2/pulse) as shown in Figure 3a, a transient absorption band (τ = ca. 150 ns) at around 330 nm decays rapidly and the 350 nm band remains in the spectrum monitored at a 450 ns delay after the laser excitation. When it is irradiated with an intense laser (ca. 260 mJ/cm^2/pulse) (Figure 3b), the 350 nm band appears almost

immediately after the excitation. The 330 nm band of BDO in Figure 3a is safely assigned to that of the diphenylcarbene group of reaction intermediates from the comparison with the spectrum shown in Figure 2. The peak in the transient spectra is slightly red-shifted because of the photobleaching of the absorption of the ground state BDO. The band peaked at around 350 nm is mostly attributable to the absorption of a diphenylmethyl radical group generated from the hydrogen abstraction reaction of the diphenylcarbene group, since its spectrum is very similar to that of the diphenylmethyl radical (340 nm) generated from bromodiphenylmethane and chlorodiphenylmethane. Absorption bands of the carbene and the radical are overlapped each other in the 320-480 nm region. The absorption bands in the spectra of BDO under the high laser intensity (Figure 3b) may be assigned analogously, though the absorption of the carbene group is not very apparent in the spectra (see, below). The difference in the two spectra (Figure 3a and b) indicates that the primary process of BDO is affected by laser intensity: Multiphoton process may occur under the intense laser excitation.

Laser power dependence of the transient absorption of BDO was examined in detail for the decay curves at 330 and 350 nm (Figure 4). When excited by a weak laser pulse, the decay curves monitored at 330 nm and 350 nm are composed of the fast and slow decay components, though the photobleaching of the absorption of the ground state BDO is observed in the decay curve at 330 nm. The fast component is assigned mostly to the absorption due to

the carbene group, while the slow one to the diphenylmethyl radical group (see also Figure 3). Power dependence of the absorbance of two decay components is shown in Figure 5. With increasing the laser power, the absorbance of the radical group monitored at 350 nm at a 2.5 μs delay after the laser excitation increases linearly in low laser power, and then reaches its plateau. Similarly the absorbance monitored at 330 nm at a 2.5 μs delay linearly increases with laser intensity. The slopes are about 1.1 (350 nm) and 1.0 (330 nm). In marked contrast to the power dependence of the absorbance of the radical, the absorbance of the carbene monitored at 330 nm at its maximum intensity is almost constant regardless of the laser power. Although the photobleaching of the absorption of the ground state BDO takes place at 330 nm, this unusual power dependence of the absorbance of the carbene group strongly indicates that in the intense laser excitation the considerable fraction of the diphenylcarbene group disappears via a biphotonic process within a single laser pulse.

Furthermore, the lifetime of the fast decay component is about 150 ns under the weak laser excitation and slightly increases under the intense excitation (ca. 200 ns). The absorption of a new intermediate, a biradical composed of two diphenylmethyl radicals at two ends, emerges as a fast decay component in the intense laser excitation in addition of that of the carbene group (see below).

In order to make above findings clearer, the transient spectra of DO, which has only one diazo group at the one end of the chain, was examined. As expected, the transient absorption spectra of DO in benzene under both the weak and the intense laser excitation are analogous to those of BDO under the weak laser excitation (Figure 3a). Thus, it is concluded that the spectral change shown in Figure 3 is peculiar to the bifunctional compound BDO: Two diazo groups at the ends of the chain in BDO are decomposed within a single intense laser pulse.

Magnetic field effect: An external magnetic field effect was examined on the transient absorption spectra of BDO and DO in the 320-460 nm region under both a weak and an intense laser excitation. The effect was observed, however, on the transient decay of the methyl radical generated from BDO *only* when excited by the intense laser excitation (Figure 6). In the presence of a magnetic field (0.6 T), the decay rate monitored at 350 nm becomes slower and the intensity at a 4 μs delay increases by about 13% (Figure 4). In the presence of a magnetic field, a medium decay component (τ = ca. 6 μs) appears, as will be described later.

Reaction mechanism: All the observations on BDO mentioned above can be interpreted by the reaction scheme shown in Scheme 1. Under the weak laser excitation, only one diazo group at the one end of the chain in BDO is excited, resulting in the formation of the carbene 1. 1 undergoes the cyclization reaction, generating a cyclic azin 2. 1 also undergoes hydrogen abstraction reaction

presumably from the impurity in the solvent, resulting in the formation of a radical 3. When excited with an intense laser pulse, the diazo group remained in the intermediates 1 and 3 are further photolysed. A cyclic oleffin 5 may be formed from the end-to-end cyclization of a biscarbene 4. On the other hand, a biradical 7 is considered to be formed from 6 via 3 and 4. Thus, the transient absorption shown in Figures. 3 and 4 may be explained as follows: In the weak laser excitation, the fast decay component due to the carbene group may be attributable mainly to the absorption of 1 and the slow one to the radical 3. Under the intense laser excitation, the absorption of 6 and 7 may be superimposed on the fast decay component due to 1, as the absorption bands of the carbene and the radical are overlapped each other in this region. The fact that the lifetime (200 ns) of the fast decay component under the intense laser excitation is slightly larger than under the weak excitation (150 ns) is due to the emergence of the absorption of 6 and 7.

Under the weak excitation, 2 is expected to be a major product.[9-11] An attempt to isolate it was, however, failed, most probably owing to the instability of 2. Under the intense excitation, a new product 5, which is not detectable under the weak laser excitation, was obtained. From its NMR, mass, UV and fluorescence spectral data,[12] 5 is assigned tentatively to a cyclic oleffin shown in scheme 1, though its stereochemistry is not determined in this study.

Present scheme is consistent with the preparative laser photolysis study of bisdiazomethane 1,2-bis[2-(α-diazobenzoyl)phenyl]ethane, in which photoproducts analogous to 2 and 5 were isolated with the yields of 3 and 50 %, respectively.[3]

Mechanism of magnetic field effect: The magnetic field effect observed in the photolysis of BDO under the intense excitation, is therefore, attributable to that on the biradical 7. Under the intense laser excitation, a small amount of 7 may be generated through the biphotonic process. In Figure 4b, an apparent lifetime of the fast decay component under the intense laser excitation (200 ns) is, therefore, attributable to the absorption due to 1, 6 and 7. At zero field, the lifetime of 7 is estimated to be 100-200 ns. Absorption of the long decay component is attributable to 3, whose lifetime is estimated to be as long as 200 μs. The decay curves in Figure 6 under the intense laser excitation in a magnetic field is considered to be the sum of the absorbance of 1, 3, 6, and 7, in which the lifetime of 7 is solely magnetic field dependent. By assuming that the long decay component (3) (τ = ca. 200 μs) is magnetic-field-independent, the lifetime of 7 in a magnetic field is obtained to be about 6 μs.

Initially prepared biradical 7 is a mixture of singlet and triplet spin states with the population ratio of 1:3, as the case of the recombination of two free radicals. In the absence of a magnetic field, two spin states are in dynamic equilibrium due

to the fast electron-nuclear hyperfine-induced singlet-triplet intersystem crossing and 7 decays via the end-to-end cyclization reaction in the singlet state. In the presence of a magnetic field, its triplet-singlet intersystem crossing is reduced because of the Zeeman splitting of two triplet sublevels and the increment of the biradical lifetime may occur, as observed in other chain-linked triplet biradicals.[4,6,7]

The magnetic field is also expected to influence the end-to-end recombination reaction of the biscarbene 4. The effect was, however, hardly detected in the decay of the carbene group at around 330 nm. It is mostly because the recombination of 4 is a very fast process (greater than 10^8 s^{-1}) compared with the spin conversion process in 4, as discussed in the previous section. Since the decay curves of both the carbene and radical groups do not exhibit magnetic field effect concurrently, a magnetic field seems not affect on the decay of 6, which has both the carbene and radical groups in its two ends.

In conclusion, it has become feasible to control photoreactions of a bifunctional compound BDO by the simultaneous use of laser and magnetic field.

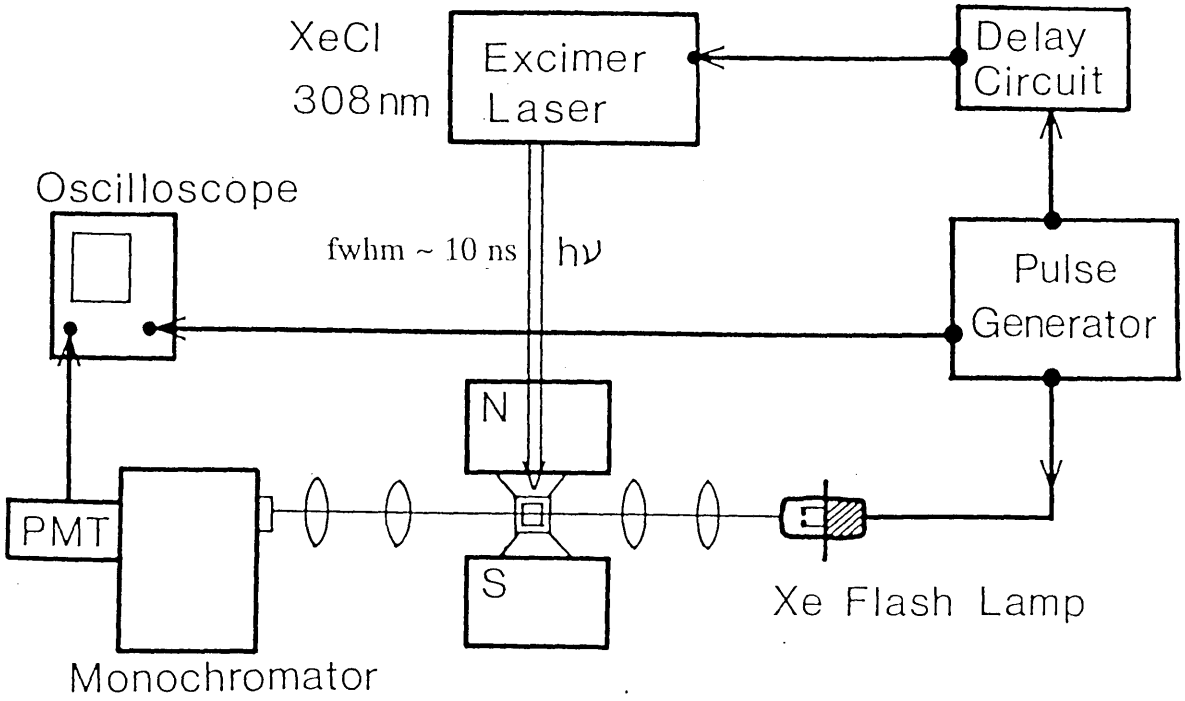

Figure 1. experimental setup of laser flash photolysis.

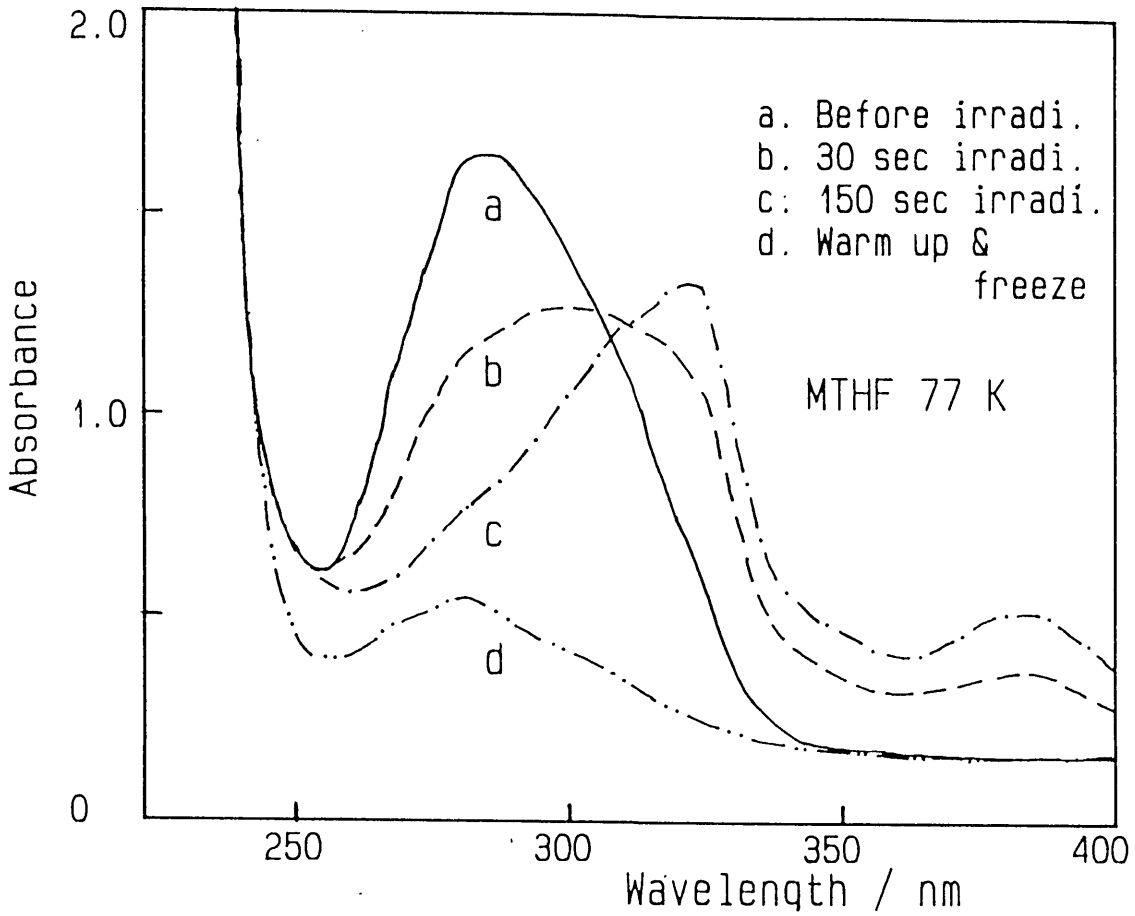

Figure 2. Absorption spectra observed by the photolysis of BDO in 2-methyltetrahydrofuran at 77K; (a) before irradiation, (b) after 30 s irradiation, (c) after 150 s irradiation, and (d) after warming up to room temperature.

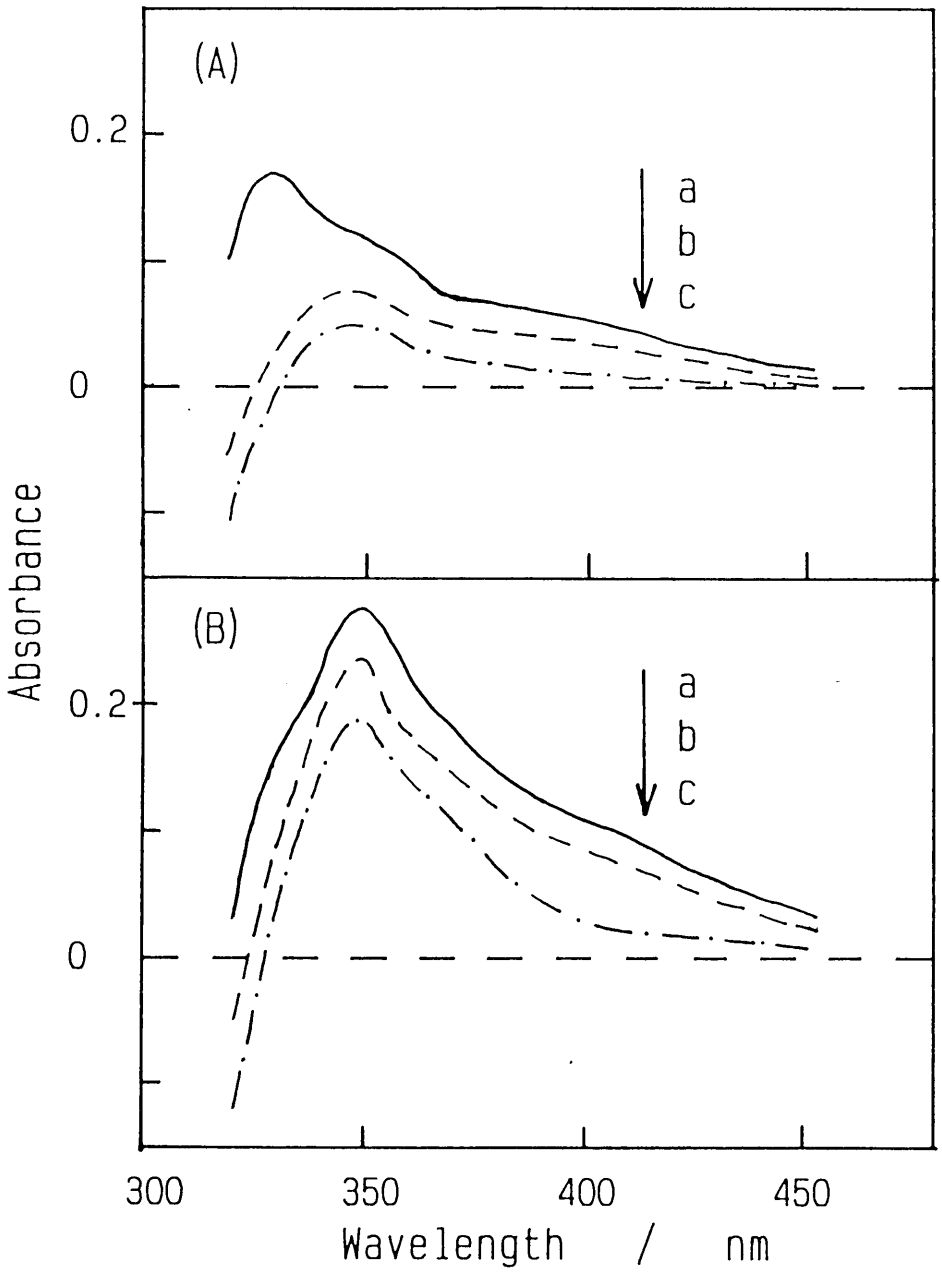

Figure 3. Transient absorption spectra of BDO in benzene under (A) a weak laser excitation (ca. 30 mJ/cm^2/pulse) and (B) an intense excitation (ca. 260 mJ/cm^2/pulse). Delaytimes after the laser excitation are (a) 100 ns, (b) 410 ns and (c) 780 ns.

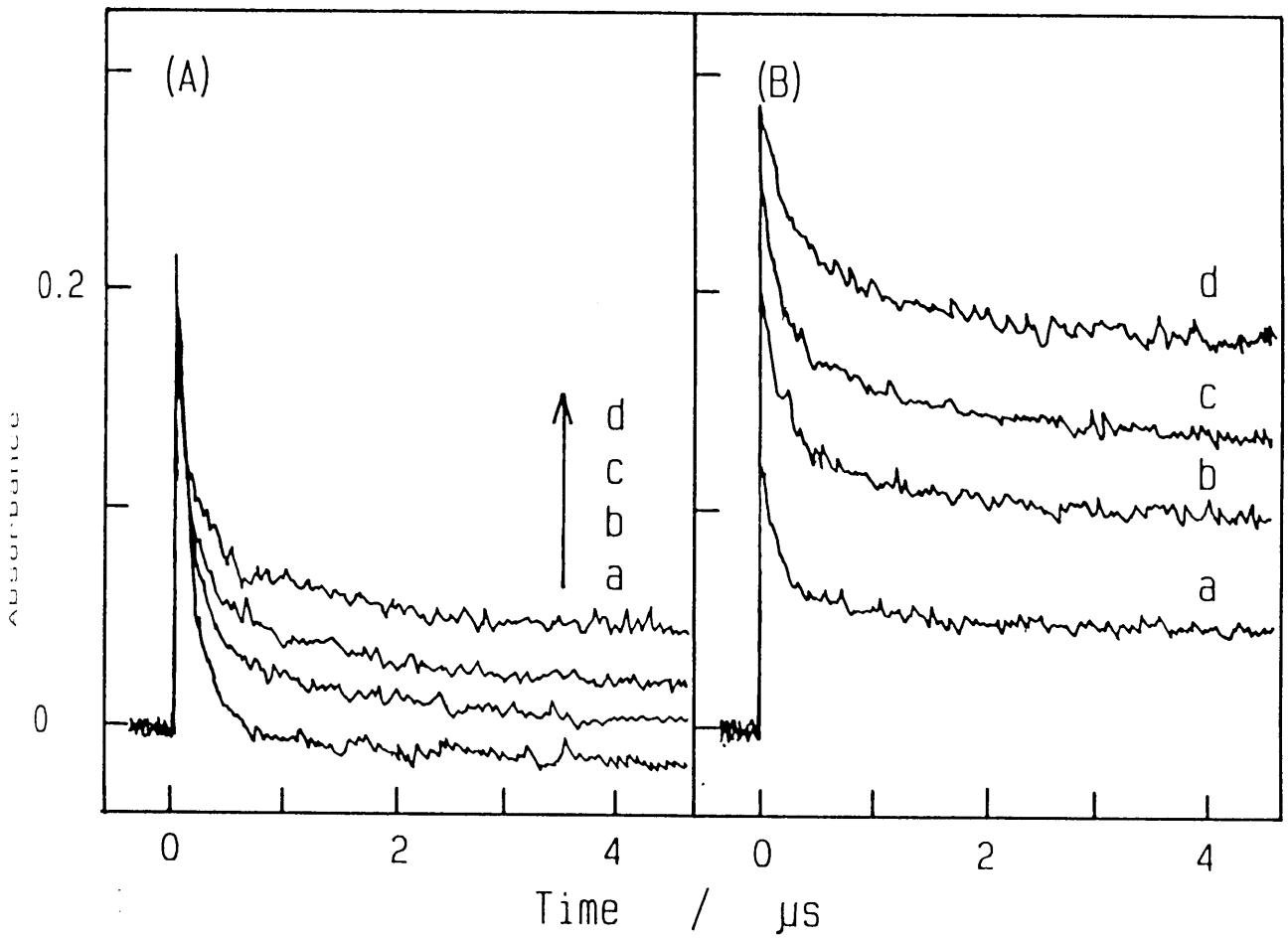

Figure 4. Effect of laser intensity on the decay curves of BDO monitored at (A) 330 nm and (B) 350 nm. Laser intensities are about (a) 30, (b) 65, (c) 100 and (d) 260 mJ/cm^2/pulse.

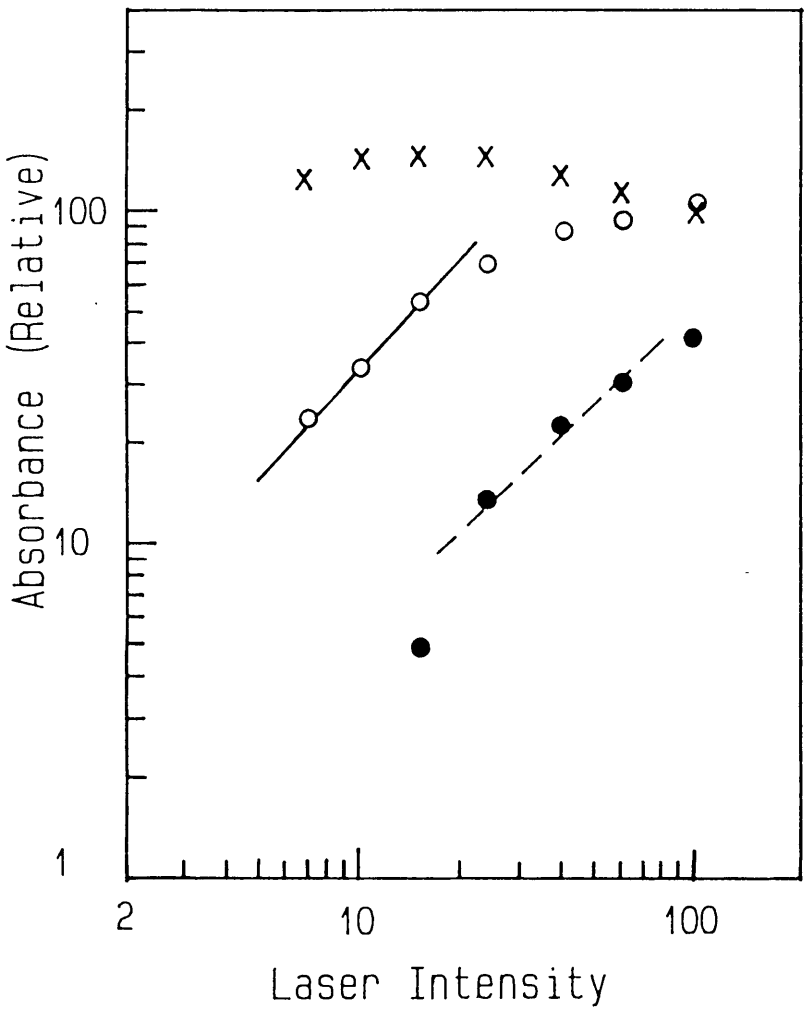

Figure 5. Laser power dependence of the intensities of transient absorption monitored at 350 nm at a 2.5 μs delay after the laser excitation (○), at 330nm at a 2.5 μ delay (●), and at 330 nm at its peak intensity (X). A 100 % relative intensity of the laser power corresponds to the absolute intensity of about 430 mJ/cm^2/pulse.

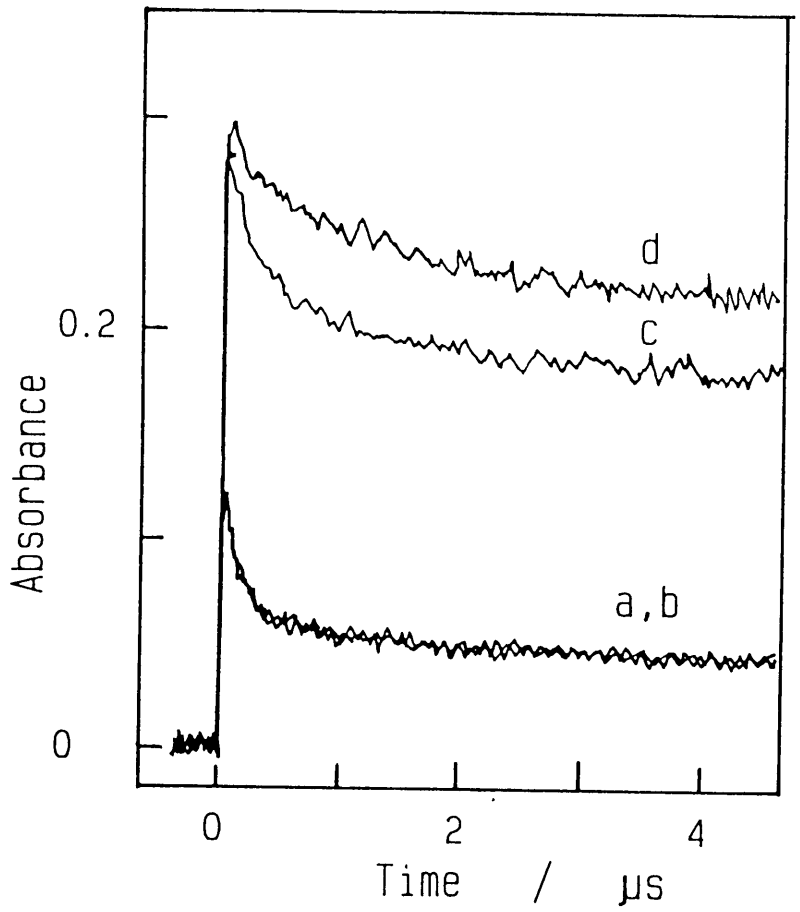

Figure 6. Magnetic field effect (0.6 T) on the decay curve of BDO at 350 nm. Laser intensities and magnetic fields are (a) 30 mJ/cm^2/pulse and 0 T, (b) 30 mJ/cm^2/pulse and 0.6 T, (c) 260 mJ/cm^2/pulse and 0 T, (d) 260 mJ/cm^2/pulse and 0.6 T.

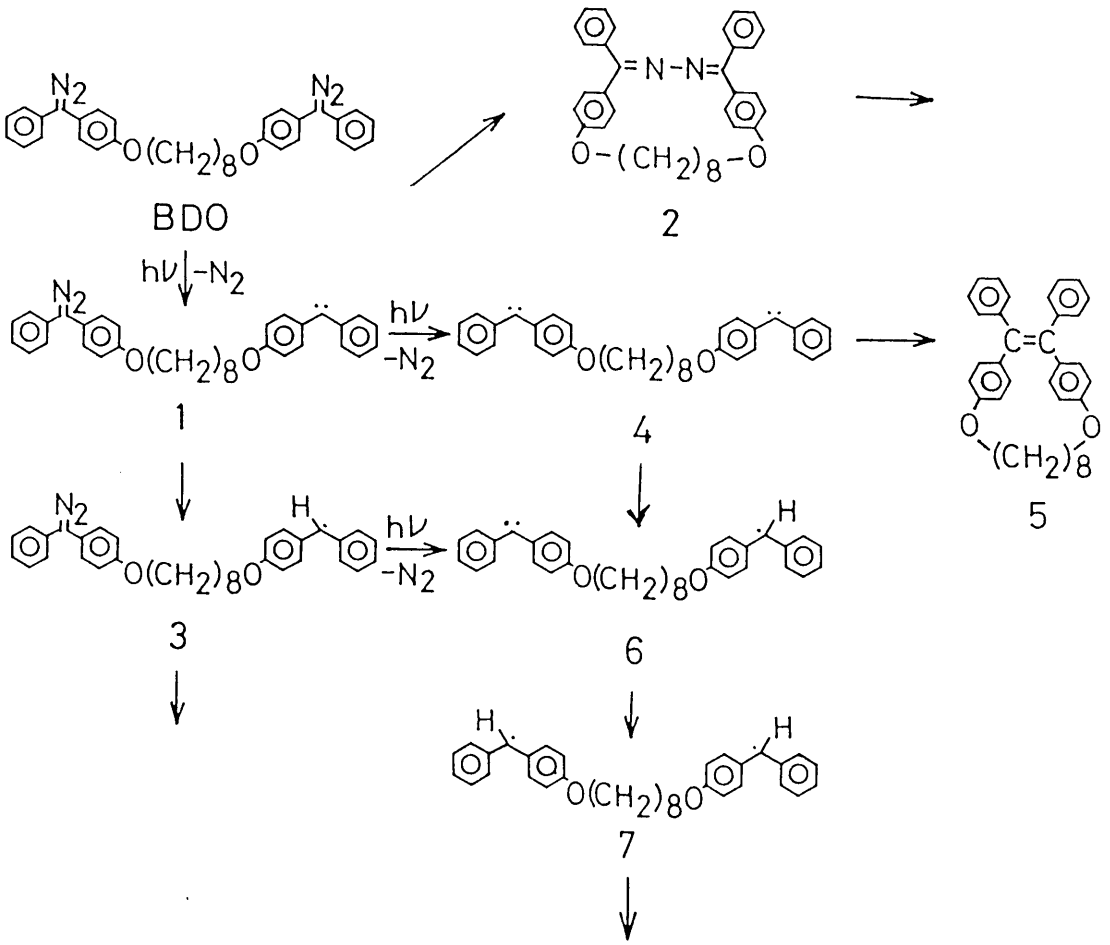

Scheme 1.

References and Notes

(1) Turro, N. J.; Aikawa, M.; Butcher, Jr. J. A.; Griffin, G. W. *J. Am. Chem. Soc.*, 1980, *102*, 5127.

(2) For reviews, see; Turro, N. J.; Ramamurthy, V.; Cherry W.; Farneth, W. *Chem. Rev.*, 1978, *78*, 125. Scaiano, J. C.; Johonston, L. J.; McGimsey W. G.; Weir, D. *Acc. Chem. Res.*, 1988, *21*, 22.

(3) Hannemann, K.; Wirz, J. *Angew. Chem. Int. Ed. Engl.*, 1988, *27*, 853.

(4) For reviews, see: Doubleday, Jr. C.; Turro, N. J.; Wang, J.-F. *Acc. Chem. Res.*, 1989, *22*, 199; Tanimoto, Y. In "Trends in Physical Chemistry 1", Council of Scientific Research Integration (Ed.), Research Trends, Trivandrum, 1991, p.79.

(5) Weller, A.; Staerk, H.; Treichel, R. *Faraday discuss. Chem. Soc.*, 1984, *78*, 271.

(6) Zimmt, M. B.; Doubleday, Jr. C.; Gould, I. R.; Turro, N. J. *J. Am. Chem. Soc.*, 1985, *107*, 6724.

(7) Tanimoto, Y.; Takashima, M.; Hasegawa, K.; Itoh, M. *Chem. Phys. Lett.*, 1987, *137*, 330; Tanimoto, Y.; Takashima, M.; Itoh, M. *Bull. Chem. Soc. Jpn.*, 1989, *62*, 3923.

(8) Fujiwara, Y.; Sasaki, M.; Tanimoto, Y.; Itoh, M. *J. Phys. Chem.*, 1988, *93*, 702.

(9) Giganek, E.; Krespan, C. G. *J. Org. Chem.*,1968, *33*, 541.

(10) Reimlinger, H. *Chem. Ber.*, 1964, *97*, 3503 ; *Chem. Ind.*,

1966, 1682.

(11) Schonberg, A.; Frese, E. *Tetrahedron Lett.* 1964, 2575.

(12) Spectral data of product 3 are as follows. ^{1}H-NMR($CDCl_3$) δ 1.26 (12H, s, $-CH_2-$) 3.98 (4H, t, $-OCH_2-$), 6.5-7.1 (18H, m, Ar-H); MS, m/e 474(M^+); UV(CH_3CN) λ 252, 300 nm; Fluorescence (CH_3CN) λ 480 nm. UV absorption and fluorescence spectral data of tetraphenylethylene are as follows: UV(CH_3CN) λ 236, 297 nm; Fluo.(CH_3CN) λ 480 nm.

APPENDIX

Let us consider the magnetic field effects on radical pair reactions. Figure A depicts the reaction scheme for a pair of neutral radicals when recombination is possible only from the singlet state. In the case where the pair is in the triplet state, the recombination is forbidden. However, if the pair turn into singlet within its lifetime, recombination becomes possible.

Magnetic fields have effects upon this singlet-triplet transition process. This process is most effective at interradical distance where exchange interactions can be neglected and therefore the singlet and triplet states are degenerate (more than 1 nm). In the absence of an external field, the three energy levels of a triplet are also degenerate so that S-T transition is possible between a singlet and three individual triplet sublevels by electron-nucler hyperfine interactions[1] (see Figure B (a)). In the presence of an external field, the energy levels of a triplet are split by the Zeeman interaction into three sublevels (T_+, T_0, and T_-) in accordance with the three possible projections of the overall spin on the external field direction (+1, 0, -1) (see Figure B (b)). The magnitude of this splitting equals $g\beta H$ where g is the electron g-value, β is the Bohr magneton, and H is the magnetic field strength. Consequently, T_+ - S and T_- - S transitions become impossible and therefore total intersystem crossing rate will be suppressed.

In the case where the initially prepared radical pair is a

mixture of singlet and triplet spin states with a population ratio of 1:3, a portion of singlet pairs recombines immediately but triplet pairs remain. In the presence of a magnetic field, the triplet pairs accumulate because only T_0 - S transition is possible but T_+ - S and T_- - S transitions become impossible. This is the reason why the lifetime of biradical increases with magnetic field.

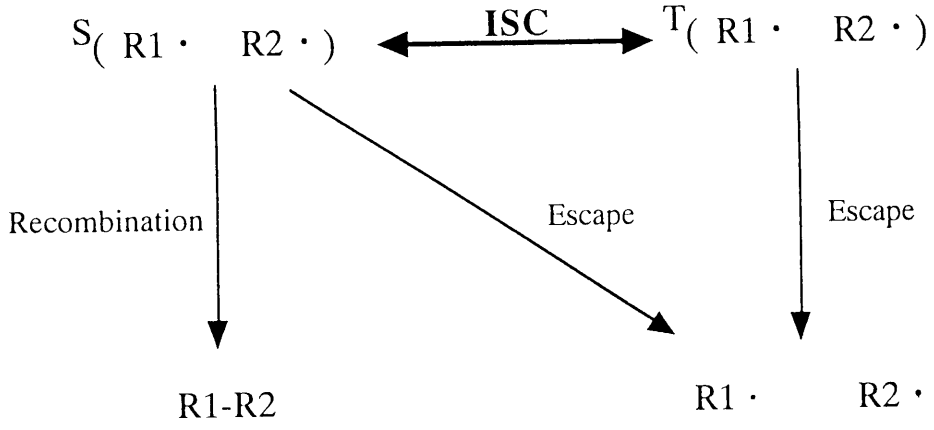

Figure A. Scheme of processes of in-cage radical pair recombination

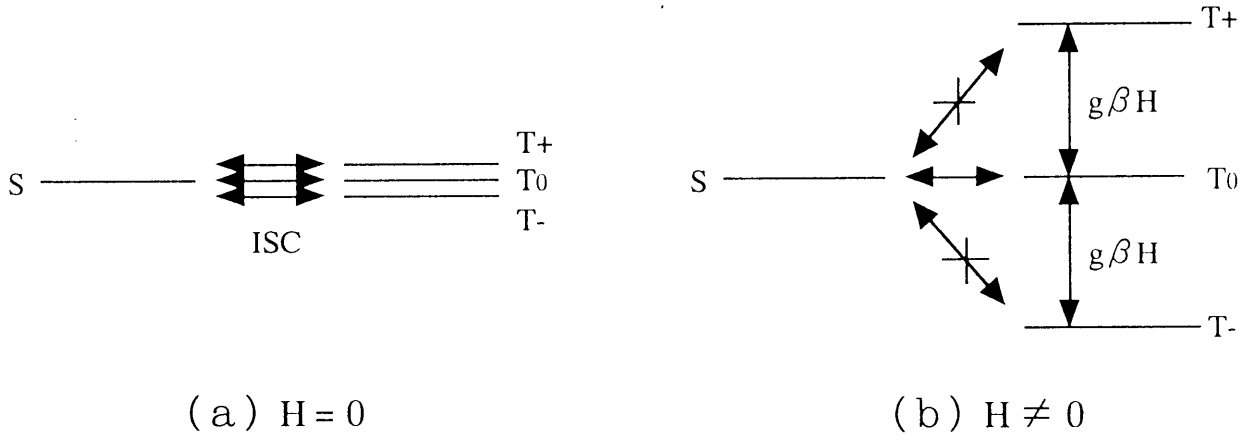

Figure B. Scheme of intersystem crossing in the absence (a) and presence (b) of external magnetic fields.

LIST OF COMPOUNDS

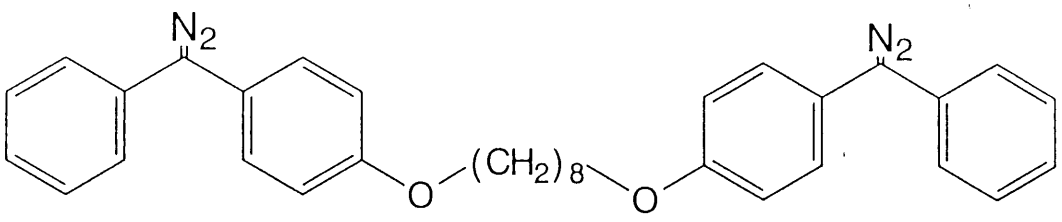

1,8-bis [4-(α-diazobenzoyl)phenoxy]octane (BDO)

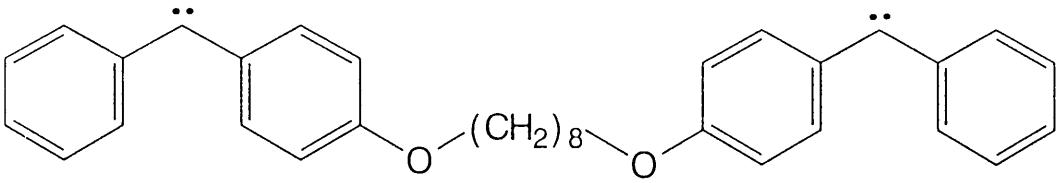

biscarbene

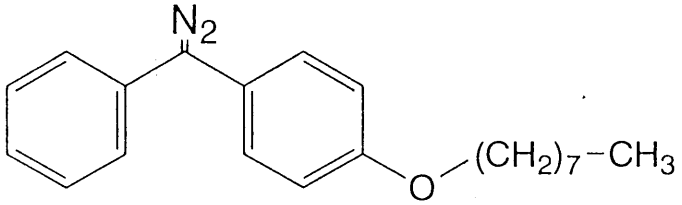

1- [4-(α-diazobenzoyl)phenoxy]octane (DO)

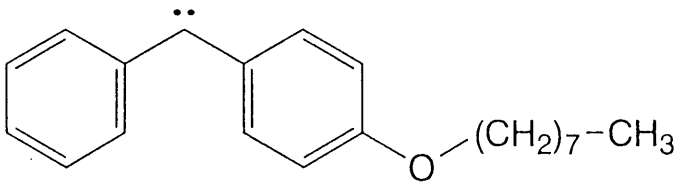

monocarbene

SUMMARY

SUMMARY

Intermolecular multiplet-multiplet energy transfer and photochemical reactions of aromatic free radicals and carbenes were examined by means of time-resolved fluorescence spectroscopy and laser flash photolysis. Numerous investigations on the electronic energy transfer between the excited and ground state molecules with the same spin multiplicity have been reported. The singlet-singlet excitation energy transfer is essentially based on the theory of the transition dipole-dipole interaction by Förster and others, while the triplet-triplet energy transfer is attributable to the electron exchange interaction developed by Dexter and others. In this thesis, unusual electronic energy transfer in the different spin multiplicities, i.e. from the singlet excited state to the doublet state of 2,4,6-tri-*tert*-butylphenoxyl radical (TBPR) and from the triplet excited state of diphenylcarbene (DPC) to the stable singlet molecules, have been investigated. Further, the photochemical reaction of the bis-carbene precursor was examined from the viewpoint of the effects of excitation intensity and magnetic fields.

The outlines of this thesis are as follows: (1) The mechanism for the energy transfer from dye molecules to TBPR as well as that from DPC to dye molecules were characterized as the resonance dipole-dipole interaction. The applicability of the Förster theory for the resonance energy transfer systems involving aromatic free radicals and carbenes was demonstrated. (2) The energy transfer analysis was available for the

characterization of the sublevels of the lowest excited triplet state (T_1) of DPC. It was confirmed that the biexponential fluorescence decays of DPC is mainly caused by the different intersystem crossing rates from the corresponding sublevels of T_1 to lower energy singlet states. This result indicates that spin-orbit coupling influences intersystem crossing, but not radiative process. (3) The effects of pulsed laser intensity and magnetic fields on the primary photochemical process in 1,8-bis[4-(α-diazobenzoyl)phenoxyl]octane (BDO) was recognized. On the high density laser excitation, two diphenylcarbene moieties on the ends of alkyl chain (bis-carbene) were simultaneously generated from BDO. The magnetic field effect was observed on the radical pair generated by subsequent hydrogen abstraction reaction of bis-carbene.

An interesting prospect is expected to be developed by the conclusion (2). The energy transfer analysis for obtaining two distinct fluorescence quantum yields, radiative and nonradiative rate constants might be useful for elucidating excited state deactivation processes in which two fluorescence components cannot be resolved in fluorescence spectra, e.g. tautomers in equilibrium. Thus, this method may contribute to the development of the excited state photophysics on such complicated systems which cannot be solved by means of the conventional method.

ACKNOWLEDGEMENT

ACKNOWLEDGEMENT

The author is indebted to Professor Michiya Itoh for his helpful discussions, suggestions and his encouragements during this work. He also wishes to express sincere gratitude to Professor Yoshifumi Tanimoto (Hiroshima Univ.) for giving me the opportunity of this work and his valuable suggestion. He is also indebted to Associate Professor Ryoichi Nakagaki for the advice and invaluable discussions. He is also grateful to Dr. Tomiki Ikeda (Research Laboratory of Resources Utilization, Tokyo Institute of Technology) for his helpful suggestions and support on fluorescence measurements. For the valuable comments on this manuscript, he is obliged to Dr. Kunihiro Tokumura. He is also very greatful to Mr. O. Oyama who arranged the program software to analyze decay curves. He also wishes to express his gratitude to Miss Masako Murata and Miss Chizuko Sugita for the help in parts of this work.

LIST

OF

PUBLICATION AND SUB-PUBLICATION

LIST OF PUBLICATION

(1) Title : Laser Flash Photolysis Study of the Primary Process in 1,8-Bis[4-(&A-diazobenzoyl)phenoxy]octane: Effect of Laser and Magnetic Field (Tanimoto, Y.; Nagano, M.; Fujiwara, Y.; Kohtani, S.; Itoh M. *J. Photochem. Photobiol. A: Chem.* 1993, *74*, 153)

(2) Title : Resonance Energy Transfer from the Excited Singlet State of Dye Molecules to a Stable Free Radical (Kohtani, S.; Murata, M.; Itoh M. *Chem. Phys. Lett.* 1995, *247*, 293)

(3) Title : Resonance Energy Transfer from the Lowest Excited Triplet State of Diphenylcarbene to Dye Molecules: Utilization to Characterization of the Triplet-Triplet Fluorescence (Kohtani, S.; Sugita C.; Itoh M. *J. Phys. Chem.* 1996, *100*, 17735)

LIST OF SUB-PUBLICATION

(1) Title : Spectral Sensitization of a TiO_2 Semiconductor Electrode by CdS Microcrystal and its Photoelectrochemical Properties (Kohtani, S.; Kudo, A.; Sakata, T. *Chem. Phys Lett.* 1993, *206*, 166)

(2) Title : Picosecond and Two-Step LIF Studies of the Excited-State Proton Transfer in 3-Hydroxyxanthone and 7-Hydroxyflavone Methanol Solution: Reinvestigation of Tautomer and Anion Formations (Mukaihata, H.; Nakagawa T.; Kohtani S.; Itoh M. (*J. Am. Chem. Soc.* 1994, *116*, 10612)

(3) Title : Picosecond Fluorescence and Two-Step LIF Studies of the Excited-State Proton Transfer in Methanol Solution of 7-hydroxyquinoline and Methyl-Substituted 7-Hydroxyquinolines (Nakagawa, T.; Kohtani S.; Itoh M. *J. Am. Chem. Soc.* 1995 *117*, 7952)

(4) Title : Photodissociation of Jet-Cooled Intramolecular Exciplex in 1-(9-Anthryl)-3-(p-(N,N-dimethylamino)phenyl)propane: Formation of Excited-State Anthryl and Deuterated Effect (Kurono, M.; Mitsuhashi, C.; Kohtani, S.; Itoh, M. *J. Phys. Chem. A* 1997, *101*, 481)